

4-2019

# Using Theoretical And Experimental Particle Packing For Aggregate Gradation Optimization To Reduce Cement Content In Pavement Concrete Mixtures

Miras Mamirov

*University of Nebraska-Lincoln*, [miras.mamirov@unl.edu](mailto:miras.mamirov@unl.edu)

Follow this and additional works at: <https://digitalcommons.unl.edu/civilengdiss>

Part of the [Civil Engineering Commons](#), and the [Other Civil and Environmental Engineering Commons](#)

---

Mamirov, Miras, "Using Theoretical And Experimental Particle Packing For Aggregate Gradation Optimization To Reduce Cement Content In Pavement Concrete Mixtures" (2019). *Civil Engineering Theses, Dissertations, and Student Research*. 136.  
<https://digitalcommons.unl.edu/civilengdiss/136>

This Article is brought to you for free and open access by the Civil Engineering at DigitalCommons@University of Nebraska - Lincoln. It has been accepted for inclusion in Civil Engineering Theses, Dissertations, and Student Research by an authorized administrator of DigitalCommons@University of Nebraska - Lincoln.

USING THEORETICAL AND EXPERIMENTAL PARTICLE PACKING FOR  
AGGREGATE GRADATION OPTIMIZATION TO REDUCE CEMENT CONTENT  
IN PAVEMENT CONCRETE MIXTURES

by

Miras Mamirov

A THESIS

Presented to the Faculty of  
The Graduate College at the University of Nebraska  
In Partial Fulfillment of Requirements  
For the Degree of Master of Science

Major: Civil Engineering

Under the Supervision of Professor Jiong Hu

Lincoln, Nebraska

April, 2019

USING THEORETICAL AND EXPERIMENTAL PARTICLE PACKING FOR  
AGGREGATE GRADATION OPTIMIZATION TO REDUCE CEMENT CONTENT  
IN PAVEMENT CONCRETE MIXTURES

Miras Mamirov, M.S.

University of Nebraska, 2019

Advisor: Jiong Hu

The main objective of this study was to evaluate the effect of aggregate particle packing optimization and cement reduction on Nebraska slip-form pavement concrete performance. A literature review was conducted to examine different aggregate optimization tools, quality control tests, and historical data of Nebraska Department of Transportation (NDOT) mixtures. It was found that the Modified Toufar Model has good potential in optimizing particle packing and predicting packing degrees. The combined void content test was found to be useful to experimentally justify optimized aggregate gradations. Two specific pavement concrete workability tests, i.e., the Box Test and the VKelly Test, were used to evaluate the effect of cement reduction and optimized aggregate gradation on pavement concrete workability. The Box Test ranking was modified to provide a more detailed and objective evaluation. Considering one of the goals of the study was to maximize the use of local materials, locally available cementitious materials and aggregates from East and West Nebraska were selected. Analysis of different aggregate combinations has shown that experimental packing from the combined void content test has a high correlation with estimated packing from the Modified Toufar Model. Results also demonstrated that the current aggregate combination is not the optimum gradation and can be improved. The experimental

program included in this study consisted of three Phases. Phase 1 focused on obtaining promising aggregate blends by maintaining the standard cement content (564 lb/yd<sup>3</sup>, 335 kg/m<sup>3</sup>). Fresh concrete properties were the main criteria to select promising blends. Phase 2 included an evaluation of performance of pavement concrete with cement content reduced by 0.5 sack (47 lb/yd<sup>3</sup>, 28 kg/m<sup>3</sup>) steps for other reference and optimized aggregate blends. Results justified that when optimum gradation is used, cement could be reduced up to 94 lb/yd<sup>3</sup> (56 kg/m<sup>3</sup>). Phase 3 is the performance evaluation phase, which included evaluating the reference mix and selected promising mixes for setting time, modulus of elasticity, free shrinkage, restrained shrinkage, and freeze/thaw resistance. Mixtures with reduced cement and optimized aggregate gradation have shown improved freeze/thaw resistance and lower shrinkage rate. Finally, a mix design improvement procedure incorporating theoretical and experimental particle packing and using excess paste-to-aggregates ratio as the control parameter was proposed. To sum up, the study has justified that the Modified Toufar Model and the combined void content test can be useful tools in aggregate gradation optimization. In order to evaluate workability of pavement concrete more accurately, the Box Test ranking was modified based on image analysis of surface and edge quality. It was also proved that mixtures with reduced cement content and optimized aggregate gradation perform better in terms of freeze/thaw resistance and shrinkage.

## ACKNOWLEDGEMENTS

I would like to express my sincere appreciation to my advisor, Dr. Jiong Hu, for his continuous support, enthusiasm, and encouragement to do research throughout my years of study.

Besides my advisor, I would like to thank my thesis committee members, Dr. Yong-Rak Kim and Dr. George Morcoux, for their passionate participation, insightful comments, and valuable advices.

I would like to thank the Nebraska Department of Transportation (NDOT) for funding the research project and providing the opportunity to study pavement concrete. Special thanks to Mr. Mick Syslo, Mr. Wally Heyen, Ms. Lieska Halsey, and other Technical Advisory Committee members for their valuable input. In addition, I want to acknowledge the support of Mr. Ben Ricceri and Lyman-Richey Corporation for donating cement and aggregates for this research. I would also thank Mr. Kevin Piper for providing aggregates from West Nebraska.

The experimental work was conducted in Materials Research Laboratory at the University of Nebraska. I would like to thank Dulitha Fredrick, Joshua Jackson, Flavia Mendonca, Arman Abdigaliyev, Joey Malloy, and Zokhidjon Salahadinov for their valuable assistance in the laboratory.

## TABLE OF CONTENTS

TABLE OF CONTENTS.....	i
LIST OF FIGURES .....	iv
LIST OF TABLES .....	vi
CHAPTER 1. INTRODUCTION.....	1
1.1 Background.....	1
1.2 Objectives .....	6
1.3 Thesis organization .....	6
CHAPTER 2. LITERATURE REVIEW .....	7
2.1 Introduction.....	7
2.2 Particle packing theories and models.....	7
2.2.1 Furnas Model .....	8
2.2.2 Aim’s and Goff’s model .....	9
2.2.3 Modified Toufar’s model.....	10
2.2.4 The Linear Packing Density Model (LPDM).....	12
2.2.5 The Compressible Packing Model (CPM) .....	13
2.2.6 Modified Andreasen and Andersen Model .....	15
2.3 Empirical gradation optimization methods.....	16
2.3.1 0.45 power chart.....	16
2.3.2 8-18 curve .....	17
2.3.3 Tarantula curve .....	18
2.3.4 Coarseness factor chart .....	20
2.4 Factors impact aggregate packing and workability of pavement concrete .....	22
2.4.1 Maximum size of aggregate.....	22
2.4.2 Gradation.....	22
2.4.3 Aggregate shape and texture .....	23
2.4.4 Microfines content .....	23
2.5 Mixture design development.....	24
2.6 Quality control tests .....	25
2.7 NDOT historical data.....	26

2.8 Summary .....	28
<b>CHAPTER 3. EXPERIMENTAL PROGRAM.....</b>	<b>30</b>
3.1 Introduction.....	30
3.2 Materials .....	30
3.2.1 Cement and cementitious materials .....	30
3.2.2 Aggregates .....	31
3.2.3 Chemical admixtures .....	34
3.3 Combined aggregate void content test .....	35
3.4 Concrete mixing.....	37
3.5 Fresh concrete tests .....	38
3.5.1 Slump test.....	38
3.5.2 Air content test.....	38
3.5.3 Setting time test.....	39
3.5.4 Box Test.....	40
3.5.5 VKelly Test.....	45
3.6 Specimen casting and curing .....	46
3.7 Hardened concrete tests .....	46
3.7.1 Compressive strength test .....	46
3.7.2 Flexural strength test.....	47
3.7.3 Static modulus of elasticity test .....	48
3.8 Durability tests.....	48
3.8.1 Freeze/thaw resistance .....	48
3.8.2 Surface and bulk resistivity.....	49
3.8.3 Free shrinkage.....	50
3.8.4 Restrained shrinkage.....	51
<b>CHAPTER 4. EXPERIMENTAL DESIGN AND RESULTS.....</b>	<b>53</b>
4.1 Introduction.....	53
4.2 Aggregate system evaluation and selection .....	54
4.2.1 Experimental packing results .....	54
4.2.2 Theoretical packing results .....	56
4.3 Testing matrix development .....	58
4.4 Excess Paste/Aggregates Calculation .....	60
4.5 Phase 1 Results .....	61
4.5.1 Mix proportions .....	61
4.5.2 Fresh concrete properties .....	62

4.6 Phase 2 Results .....	64
4.6.1 Mix proportions .....	64
4.6.2 Fresh concrete properties .....	65
4.7 Hardened concrete properties of Phases 1 and 2.....	70
4.8 Performance evaluation .....	72
4.8.1 Mix proportions .....	72
4.8.2 Fresh concrete and mechanical properties .....	73
4.8.3 Durability properties .....	74
4.9 Proposed changes in NDOT specifications.....	78
4.10 Summary .....	79
<b>CHAPTER 5.    MIX DESIGN IMPROVEMENT PROCEDURE.....</b>	<b>81</b>
5.1 Introduction.....	81
5.2 Design philosophy .....	81
5.3 Proposed mix design improvement procedure.....	84
5.4 Summary .....	85
<b>CHAPTER 6.    CONCLUSIONS AND FUTURE STUDIES.....</b>	<b>87</b>
6.1 Conclusions.....	87
6.2 Recommendations for Future Studies .....	88
6.2.1 Incorporation of additional parameters in mix design .....	88
6.2.2 Scientific pavement concrete workability test .....	90
<b>REFERENCES .....</b>	<b>93</b>



## LIST OF FIGURES

Figure 1.1. Annual CO <sub>2</sub> emissions from cement production (Andrew, 2018) .....	1
Figure 1.2. Comparison of shrinkage of aggregate, paste and concrete. ....	2
Figure 1.3. Illustration of cement content reduction through aggregate gradation optimization .....	3
Figure 1.4. Aggregate sources in Nebraska and Iowa .....	5
Figure 2.1. Wall effect and loosening effect (De Larrard 1999) .....	9
Figure 2.2. Correlation between predicted and experimental packing degrees (Goltermann, 1997).....	12
Figure 2.3. Compaction index versus packing degree (De Larrard, 1999).....	15
Figure 2.4. 0.45 power chart .....	17
Figure 2.5. IPR chart with ‘8-18’ limits.....	18
Figure 2.6. Tarantula curve .....	19
Figure 2.7. Coarseness factor chart.....	21
Figure 2.8. Nebraska gradations on Tarantula curve .....	27
Figure 2.9. Nebraska gradations on 8-18 curve .....	27
Figure 2.10. Nebraska gradations on Shilstone chart .....	28
Figure 3.1. Nebraska aggregates gradations .....	32
Figure 3.2. Selected aggregates .....	33
Figure 3.3. Gradation curve of aggregates used in this curve.....	34
Figure 3.4. Combined void content test .....	36
Figure 3.5. Vibration plus pressure method sketch.....	37
Figure 3.6. Slump test setup.....	38
Figure 3.7. Air pressure meter .....	39
Figure 3.8. Setting time test setup.....	40
Figure 3.9. Box test setup .....	41
Figure 3.10. Comparison of surface voids of box test rankings from different methods .	42
Figure 3.11. Examples of Box test results with different edge holding abilities .....	44
Figure 3.12. VKelly test.....	46
Figure 3.13. Compressive strength test setup .....	47
Figure 3.14. Flexural strength test setup.....	48
Figure 3.15. Static Modulus of Elasticity test setup .....	48
Figure 3.16. Setup used for freeze/thaw resistance test.....	49
Figure 3.17. Resistivity test setup .....	50
Figure 3.18. Length comparator used for shrinkage measurement.....	51
Figure 3.19. Restrained shrinkage test setup .....	52
Figure 4.1. Results of the combined aggregate void content test .....	55
Figure 4.2. Comparison between experimental and theoretical packing degrees of East NE blends.....	57
Figure 4.3. Comparison between experimental and theoretical packing degrees of West NE blends.....	58

Figure 4.4. Reference blend and blends chosen for further study plotted on Tarantula curve.....	59
Figure 4.5. Mix identification .....	62
Figure 4.6. Box test images from Phase I mixes.....	64
Figure 4.7. Box test images for East NE mixes .....	68
Figure 4.8. Box test images for West NE mixes.....	69
Figure 4.9. Effect of cement content on mechanical properties .....	71
Figure 4.10. Effect of cement content on permeability .....	72
Figure 4.11. Modulus of elasticity of reference and promising mixes .....	74
Figure 4.12. Freeze/thaw resistance results up to 120 cycles .....	76
Figure 4.13. Free shrinkage results up to 14 days.....	77
Figure 4.14. Restrained shrinkage results .....	78
Figure 5.1. Correlation among $P_c\%/V_{B\_agg}\%$ , $V_{index}$ and surface voids .....	82
Figure 5.2. Effect of $P_c\%/V_{B\_agg}\%$ ratio on surface voids .....	83
Figure 5.3. The proposed mix design improvement procedure .....	85
Figure 6.1. AIMS 2 setup.....	90
Figure 6.2. Direct measurement of aggregate shape and texture .....	90
Figure 6.3. Representation of Bingham model (Ferraris et al., 2017) .....	91
Figure 6.4. Sketch of potential new tests using rheometer and applied vibration .....	92

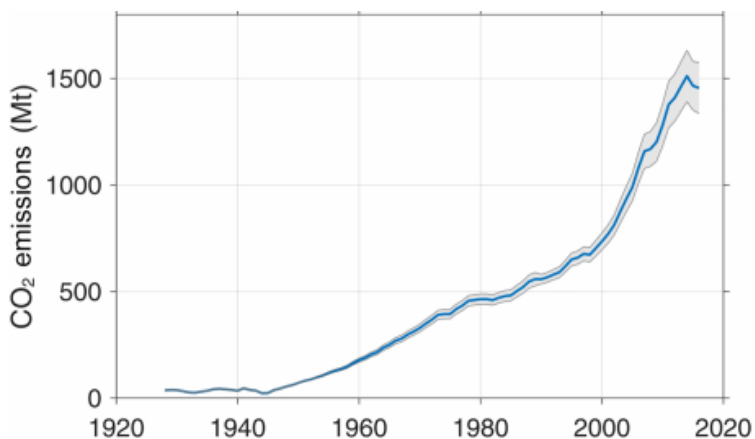
## LIST OF TABLES

Table 2.1. Compaction Index with different packing processes .....	14
Table 3.1. Chemical composition and physical properties of IP cement.....	31
Table 3.2. Aggregates properties .....	34
Table 4.1. Mix proportions for mixes of Phase 1 .....	62
Table 4.2. Fresh concrete properties of Phase 1 mixes.....	63
Table 4.3. Mix proportions for mixes of Phase 2 .....	65
Table 4.4. Fresh concrete properties of Phase 2 East NE mixes.....	67
Table 4.5. Fresh concrete properties of Phase 2 West NE mixes .....	67
Table 4.6. Mix proportions for performance evaluation mixes .....	73
Table 4.7. Fresh concrete properties of performance evaluation mixes .....	73
Table 4.8. NDOT specifications for pavement concrete mix (2017).....	79

## CHAPTER 1. INTRODUCTION

### 1.1 Background

Pavement concrete is one of the most widely used infrastructural materials with applications in highways, airports, streets, and roads. The optimization of pavement concrete mixtures is becoming essential as the industry is committing to promote economical and sustainable designs. The purpose of optimization is mainly to reduce cement, which is the most expensive ingredient in concrete and the largest contributor to carbon dioxide emissions. Recent estimates have shown that cement production contributes about 5% of total global CO<sub>2</sub> emissions (Andrew, 2018); the CO<sub>2</sub> emissions contributed by cement production are gradually increasing (Figure 1.1).



**Figure 1.1. Annual CO<sub>2</sub> emissions from cement production (Andrew, 2018)**

Shrinkage-induced cracking has been a major contributor of pavement concrete durability issues. As the shrinkage of aggregates is negligible, shrinkage of concrete, which is largely determined by cement paste, can be reduced consequently through mixture optimization. Figure 1.2 shows the comparison of shrinkage of different

materials over their drying period. Reduction of cement content can lead to a more durable concrete. As cement is also the most costly ingredient in concrete, by reducing the cement content, more cost-effective concrete pavement can be achieved.

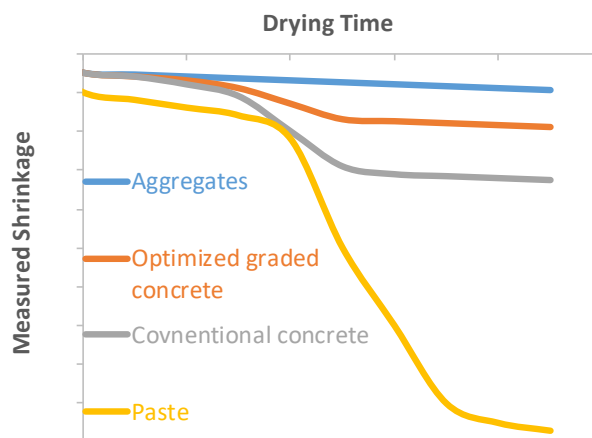


**Figure 1.2. Comparison of shrinkage of aggregate, paste and concrete.**

The most common approach to reducing cement content is to improve the particle packing of the aggregate skeleton that consists of fractions of particles at different sizes, shapes, and textures. In general, aggregates occupy around 70-80% of the concrete mixture by volume. Optimization of particle packing aims to achieve as dense a matrix as possible, i.e. with the lowest possible amount of voids in between particles. Figure 1.3 illustrates the reduced cement content with optimum aggregate gradation. It can be observed that the lower the amount of voids, the less cement paste is needed to fill them. This, in turn, resulted in a higher amount of excess paste which is then available to provide sufficient workability and bonding to ensure adequate concrete strength.

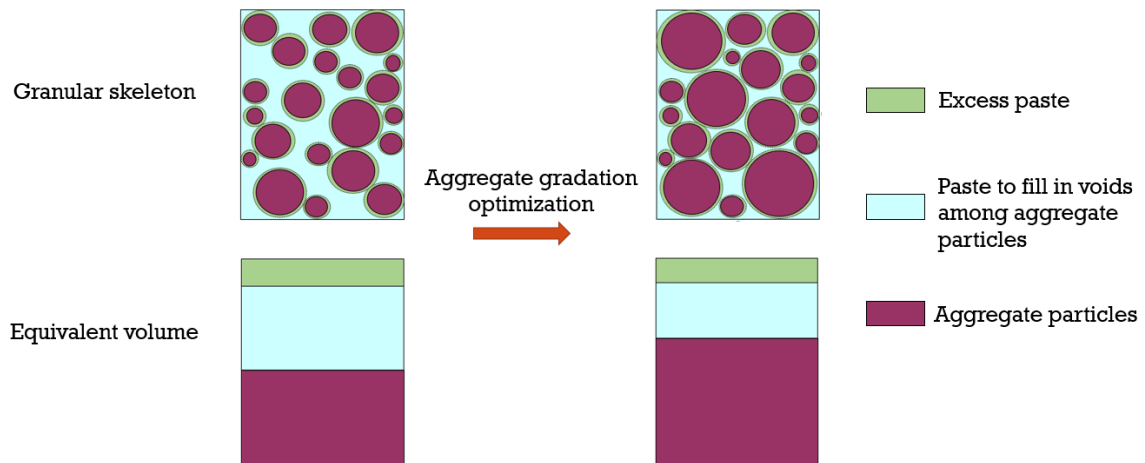


**Figure 1.3. Illustration of cement content reduction through aggregate gradation optimization**

There are many different aggregate optimization approaches currently being used in the concrete arena. Researches showed that aggregate proportioning techniques such as the 45 Power Chart, Shilstone Chart, and 8-18 Chart do not necessarily provides the lowest void content (Ley et al., 2012; Obla et al., 2007; Quiroga et al., 2004) and might not be the best tool to obtain aggregate blends for slip-form pavement mixtures (Taylor et al., 2015). A newly developed Tarantula Curve is a modified version of the 8-18 chart with adjusted upper and lower limits at different aggregate sizes (Ley et al., 2014) created based on a large amount of empirical data from hundreds of mixes. While the Tarantula Curve is likely the most recognized gradation for pavement concrete and has been adopted by many agencies and contractors, like other aggregate optimization methods, the biggest issue of the methods mentioned above is that none of them accounts for the shape and texture of aggregates. Furthermore, although methods including the Tarantula Curve can likely distinguish whether a gradation is good or bad, these approaches do not provide information on which blend is exactly the optimum one and what the packing

degree is. Due to this limitation, these methods can serve as a supplemental tool in concrete mix design, but are not adequate in guiding the gradation optimization process. It is believed that the use of necessary particle packing models, such as discrete theoretical models, can be useful. Besides obtaining optimum proportions, such models are capable of predicting the particle packing degree. Moreover, due to the fact that modeling inputs required factors such as individual packing of aggregates, these models indirectly account for aggregate shape and texture. Previous studies have shown that the Modified Toufar Model has a positive correlation between experimental and estimated packing degrees. It is believed that by using the Modified Toufar Model to determine an optimum packing, accompanied by experimental testing of the actual void content of the aggregate, a simple and more effective guidance for aggregate optimization and concrete mix design can be obtained.

Nebraska is known for its unique type of aggregates for concrete. A considerable proportion of the aggregate used is a combination of sand and gravel that is mostly fine aggregate yet with a small portion of particles within the coarse aggregate size range; further, a relatively small amount (approximately 30%) of limestone is generally used as coarse aggregate. The small amount of limestone implies a less expensive total cost of aggregate and a lower amount of angular aggregates in the design, which generally results in a relatively high pavement concrete workability compared to other states. More importantly, the combined aggregate gradation could be compromised, which leads to a higher cement content required for the concrete mixture. Current specification requires a minimum of 564 lb/yd<sup>3</sup> (335 kg/m<sup>3</sup>) of cement content for pavement concrete.

Figure 1.4 represents aggregate sources in the state of Nebraska and Iowa. As shown in the figure, there is a lack of limestone sources in West Nebraska, making granite and dolomite the more widely used coarse aggregate in that region. Granite and dolomite might significantly differ from limestone in terms of gradation, shape, and texture. While sand and gravel is used throughout the state of Nebraska, it is also important to note that sand and gravel aggregate is typically coarser in West Nebraska. Therefore, it is critical to use an effective aggregate gradation optimization tool that can be applied to different types and sizes of aggregates.

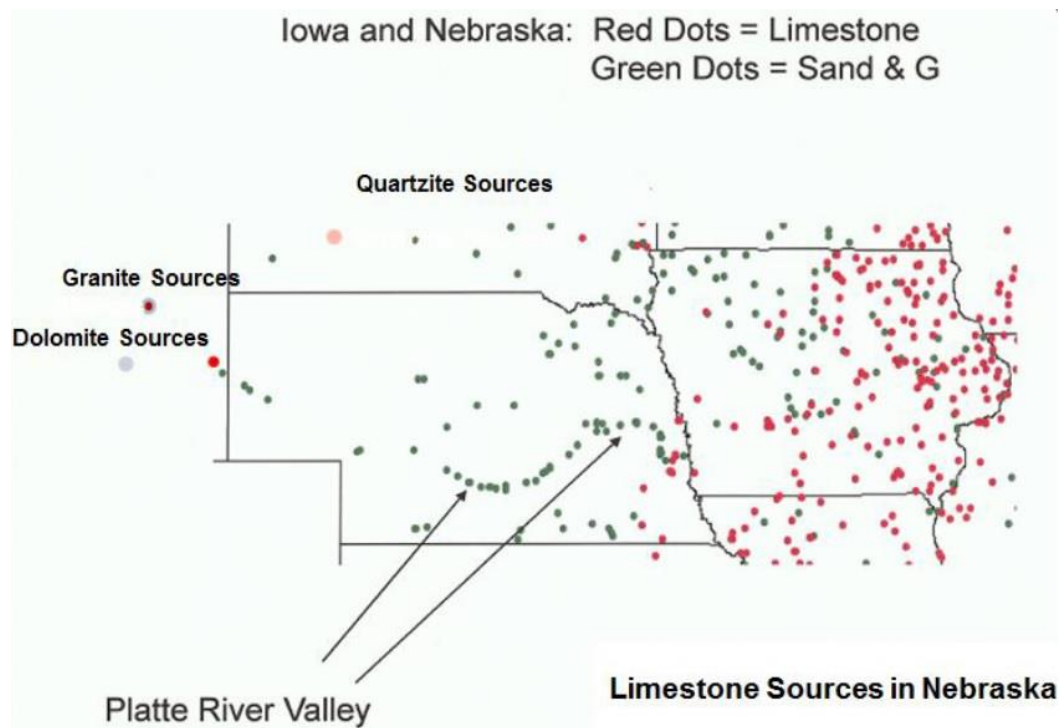


**Figure 1.4. Aggregate sources in Nebraska and Iowa**

To ensure successful concrete optimization, it is important to adopt specific tests to examine slip-formed pavement concrete workability. The Box Test and VKelly Test were developed by Cook et al. (2014) and Taylor et al. (2012), respectively, with the



purpose of evaluating fresh pavement concrete behavior under vibration. It is believed that both tests have to be examined for applicability in Nebraska where low coarse aggregate concrete mixtures are being used. Moreover, the possibility of improving test rankings should be discussed and attempted.

## 1.2 Objectives

Besides developing an effective mix design improvement method based on both theoretical and experimental packing and fresh concrete performance, the main objective of this work is to develop concrete designs for pavement applications in Nebraska with reduced cement content through aggregate gradation optimization. Therefore, historical data and information of Nebraska aggregate availability and gradation have to be collected and analyzed. The study provides recommended pavement concrete mixtures to ensure workability and constructability so that the mixes can be easily used in engineering application and appropriate mechanical properties and durability characteristics meet the Nebraska Department of Transportation (NDOT) specifications.

## 1.3 Thesis organization

The thesis is divided into seven chapters. Chapter 1 is an introduction, where the general background and main objectives are provided. A literature review is presented in Chapter 2, which includes a summary of different theoretical and empirical particle packing models and gradation optimization tools, factors affecting aggregate packing, and workability (quality control) tests of pavement concrete to justify optimized aggregate gradation. Chapters 3 to 5 include the main experimental program and results covering both East and West Nebraska aggregates. Chapter 6 summarizes all conclusions and provides recommendations for future studies.

## CHAPTER 2. LITERATURE REVIEW

### 2.1 Introduction

There are many different approaches to optimize particle packing including empirical methods, theoretical models, and experimental tests. In order to select the most effective method for this particular study in terms of optimization and prediction of the particle packing degree, a comprehensive literature review was conducted. Various theoretical models and empirical optimization tools were evaluated for their advantages, limitations, and simplicity. Besides this, factors impacting aggregate gradation and workability of pavement concrete such as maximum size of aggregate, gradation, aggregate shape and texture, and microfines content were discussed. Quality control tests to justify optimized aggregate gradation were also presented. Moreover, mixture design development for pavement concrete proposed by other researchers is discussed. Finally, NDOT historical data was presented, and it was determined that the majority of the blends currently used in the state are not optimum.

### 2.2 Particle packing theories and models

Concrete is composed of a skeleton of granular particles bound together with cementitious paste. The philosophy of particle packing is to combine grains with the lowest possible porosity to minimize the amount of binder. It is believed that the packing degree mainly depends on three parameters: particle size distribution, particle shape, and the method of processing the packing (De Larrard, 1999). There are various theories and models developed to predict particle packing of different granular matrices as accurate as possible.

### 2.2.1 Furnas Model

The first basic research on particle packing theory was conducted by Furnas (1928) in his study of the flow of gases through beds of broken solids. His discrete theory of binary system was based on the assumptions that particles are spherical in shape, small and large particles are significantly different in size (particle diameter  $d_1 \ll$  particle diameter  $d_2$ ), and small particles fill out the voids among large particles without disturbing their packing. There are two scenarios possible based on volumes of fine and coarse particles: “fine grain domain” and “coarse domain”, meaning the volume fraction of small particles is dominant and the volume fraction of large particles is dominant, respectively. The model can be described as:

$$\Phi^* = \varphi_2 + (1 - \varphi_2) * \varphi_1 \quad (2.1)$$

Where,  $\Phi^*$  is the maximum packing density of the binary system,  $\varphi_1$  and  $\varphi_2$  are individual packing densities for small and large particles respectively. If  $d_1 \approx d_2$ , the so called “wall effect” and “loosening effect” occur (Figure 2.1). The “wall effect” is a phenomenon when an isolated coarse particle in the fine particle matrix disturbs the packing and increases voids around. The “loosening effect” is when an isolated fine particle in the coarse particle matrix appears to be too large to fit in the space between coarse particles, thus disturbing the packing. If the difference in particle diameters is not significant, the  $d_1/d_2$  ratio has to be taken into consideration, which this model does not account for. Therefore, the main limitation of this model is that it does not consider the “wall effect” and the “loosening effect”.

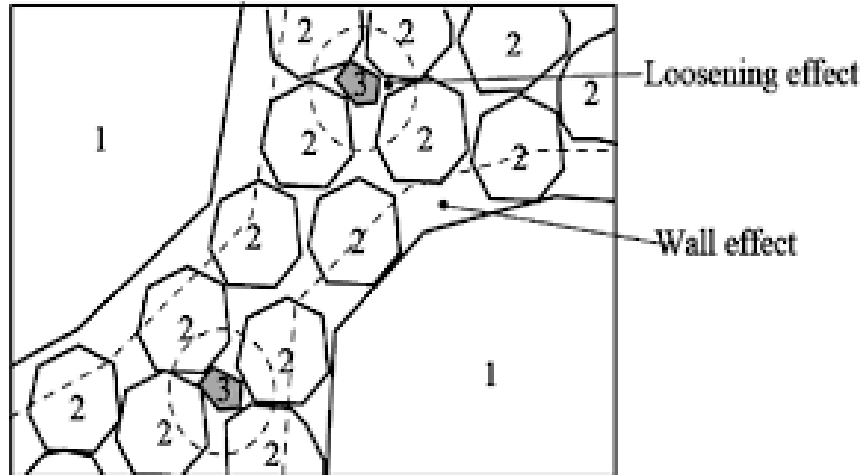


**Figure 2.1. Wall effect and loosening effect (De Larrard 1999)**

### 2.2.2 Aim's and Goff's model

According to Rudy (2009), in 1967, Aim and Goff suggested a simple geometrical model to predict the packing density of binary systems. The main improvement was that this model takes into consideration the “wall effect” in the first layer of spherical particles in contact with a smooth and plane wall. Similar to the previous model, two scenarios are considered in this method: the amount of fine particles is much less than the amount of coarse particles, or the amount of fine particles is much more than the amount of coarse particles. The first scenario implies that fine particles serve to fill the voids among coarse particles, whereas the second scenario implies that fine particles serve as a media for coarse aggregates to be embedded. The fraction of fine particles,  $V_1^*$  resulting in maximum packing density, can be calculated using the following equation:

$$V_1^* = \frac{[(\varphi_1/\varphi_2) - (1 + 0.9 * d_1/d_2) * \varphi_1]}{[(\varphi_1/\varphi_2) - (1 + 0.9 * d_1/d_2) * \varphi_1 + 1]} \quad (2.2)$$

Where,  $d_1$  and  $d_2$  are the diameters of fine and coarse particles, and  $\varphi_1$  and  $\varphi_2$  are individual experimental packing densities.  $(1 + 0.9 * d_1/d_2)$  is the factor due to wall effect, where  $d_1$  and  $d_2$  are the diameters of fine and coarse particles, respectively. The packing degree can be calculated based on two cases depending on whether the volume fraction of fine particles ( $V_1$ ) is higher or lower than  $V_1^*$ :

$$\text{For } V_1 < V_1^*, \Phi = \varphi_2 / (1 - V_1) \quad (2.3a)$$

$$\text{For } V_1 \geq V_1^*, \Phi = 1 / [(V_1/\varphi_1 + (1 - V_1) * (1 + 0.9 * d_1/d_2))] \quad (2.3b)$$

In the experimental study of Goltermann et al. (1997), this model did not correlate appropriately with the test results. It was concluded that Aim's and Goff's model cannot be used for realistic aggregates.

### 2.2.3 Modified Toufar's model

The Toufar Model is the method to design multicomponent mixtures of particles by maximizing the packing degree, which was created in the 1970's and then modified in the 1990s (Goltermann et al., 1997). The main concept implies that fine particles are not able to fill interstices between coarse particles, and, as a result, the whole matrix consists of two systems: one mostly composed of densely packed coarse particles and the other consisting of areas of packed fine particles with discretely distributed coarse particles. The main unrealistic assumptions made in this theoretical model are that 1) all particles are spherical in shape, 2) monosized, and 3) coarse and fine particles differ in size ( $d_1 \ll d_2$ ). The first two assumptions can be corrected by introducing a characteristic diameter of the aggregates and individual packing degree of the aggregates. The

characteristic diameter can be obtained by the position parameter of the Rosin-Raimmler-Sperling-Bennet distribution curve, which stands for the diameter, where 36.8% of particles are retained. Goltermann et al. (1997) stated that the characteristic diameter and individual packing degree minimize the deviations from the first two assumptions. The third assumption can cause problems in the case of overlapping fractions of fine and coarse particles with fairly different characteristic diameters. However, it was found from an experimental study that the overlapping effect has an insignificant impact on packing degree close to maximum packing or when the fraction of fine particles is high (Goltermann et al., 1997). Once the characteristic diameter and individual packing degrees are obtained, they can be used to obtain combined packing degree,  $\Phi$  as follows:

$$\Phi = \frac{1}{\left[\frac{V_1}{\varphi_1} + \frac{V_2}{\varphi_2} - V_2 * \left(\frac{1}{\varphi_2} - 1\right) * k_d * k_s\right]} \quad (2.4)$$

Where  $V_1$  and  $V_2$  are the volume fractions of fine and coarse particles respectively, and  $\varphi_1$  and  $\varphi_2$  are packing degrees of fine and coarse particles respectively.  $k_d$  is the diameter ratio factor and is calculated as  $k_d = \frac{(d_2 - d_1)}{(d_2 + d_1)}$ , where  $d_1$  and  $d_2$  are characteristic diameters of fine and coarse particles respectively, and  $k_s$  is a statistical factor. This factor was introduced after a later comparison by Goltermann et al. (1997) showed that introducing a small amount of fine particles to a sample of coarse particles does not increase the packing degree as expected. It is caused by the assumption that each fine particle placed is limited only to four coarse particles surrounding it. Introducing a statistical factor can overcome this unrealistic behavior (Goltermann et al., 1997).

$$\text{For } x < x_0, k_s = \left(\frac{x}{x_0}\right) * k_0 \quad (2.5a)$$

$$\text{For } x \geq x_0, k_s = 1 - \frac{(1+4*x)}{(1+x)^4} \quad (2.5b)$$

$$\text{Where, } x_0=0.4753, k_0=0.3881, x = \frac{(V_1/V_2)*(\varphi_1/\varphi_2)}{(1-\varphi_2)}$$

According to works of Goltermann et al. (1997), Rudy (2009), Jones et al. (2001), and Moini (2015), the Modified Toufar Method has a high correlation of theoretical and experimental packing results for binary blends of aggregates. Besides this, Goltermann et al. (1997) collected more than 800 experimental results from his own studies and other authors and compared them with the predicted packing degree (Figure 2.2). It can be seen that the Modified Toufar Model predicts packing degree very well.

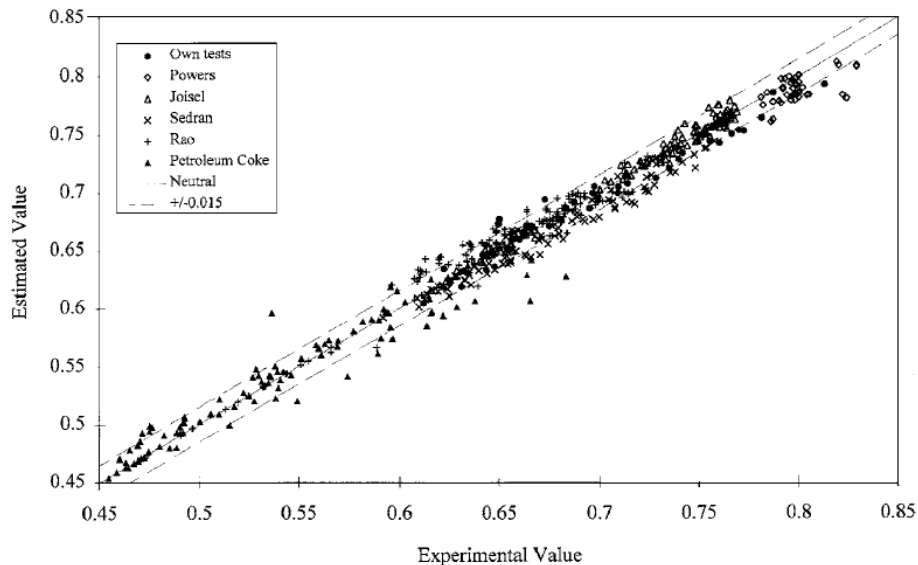


**Figure 2.2. Correlation between predicted and experimental packing degrees (Goltermann, 1997)**

#### 2.2.4 The Linear Packing Density Model (LPDM)

Stovall (1986) suggested a model for the packing density of multisized grains, where the packing density is a function of the fractional solid volume of each grain size

in the mixture. The input required to use this model includes the diameter of each grain component ( $d_i$ ), the individual packing density ( $\varphi_i$ ), and individual fractional solid volume ( $\eta_i$ ). The assumption is that grain sizes are continually distributed. The packing density of multisized grains can be calculated as the infimum, which is the lowest number in a set of numbers:

$$\Phi = \inf_{d \leq t \leq D} \left[ \frac{\varphi(t)}{1 - [1 - \varphi(t)] * \int_d^t dx * \eta(x) * g(x, t) - \int_t^D dx * \eta(x) * f(x, t)} \right] \quad (2.6)$$

Where,  $\varphi(t)$  is the packing density of the grains group with diameter  $t$  ( $d \leq t \leq D$ ), “f” and “g” are the functions of local packing disturbance due to the introduction of smaller or larger particles respectively, and can be calculated as:

$$f = \left(1 - \frac{d_i}{d_j}\right)^{3.1} + 3.1 * \left(\frac{d_i}{d_j}\right) * \left(1 - \frac{d_i}{d_j}\right)^{2.9} \quad (2.7)$$

$$g = \left(1 - \frac{d_i}{d_j}\right)^{1.6} \quad (2.8)$$

According to Mangulkar et al. (2013), LPDM is a good tool in predicting optimum proportions. However, based on the experimental study of different models by Jones et al. (2001), LPDM underestimated void ratio of binary blends of fine and coarse particles.

### 2.2.5 The Compressible Packing Model (CPM)

This model presented by De Larrard (1999) is based on the fact that the process of compaction impacts the packing density. This mathematical model is developed to predict the performance of concrete properties in the fresh and hardened stage and the



packing density of aggregates and cementitious materials (Quiroga 2004). The method allows for any number of fractions of aggregate/cementitious materials. The input required includes the mean diameter and packing density of each fraction. It was also stated that packing density is affected by the compaction method. There are several methods of compacting aggregates, such as loose placement, rodding, vibrating with or without external pressure, and wet packing. Table 2.1 presents packing processes with corresponding compaction indices. The higher the compaction index, the higher the packing degree (Figure 2.3). It can be observed that with the increase of compaction, index packing degree grows exponentially. However, no matter what compaction method is applied, ideal packing degree (1.0) cannot be reached. For coarse and fine aggregates De Larrard suggested using vibration plus 1.45 psi (10 kPa) pressure, whereas for microfines, a water demand test is suggested.

**Table 2.1. Compaction Index with different packing processes  
(According to de Larrard 1999)**

<b>Packing process</b>	<b>K</b>
Loose	4.1
Sticking with a rod	4.5
Vibrated	4.75
Vibrated + pressure	9
Wet packing	6.5

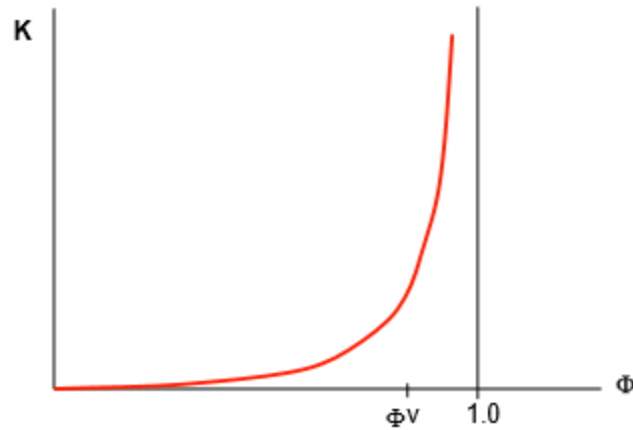


**Figure 2.3. Compaction index versus packing degree (De Larrard, 1999)**

Jones et al. (2001) analyzed the CPM for its suitability in proportioning mixtures. In the scenario of binary blends with fine and coarse fractions, the CPM overestimated the void ratio. In terms of prediction of fresh concrete performance, the CPM Model was calibrated using data of mixtures with slump more than 4 in, which implies that for stiff mixes (slump lower than 4 in), there is a high probability that CPM predictions will be inaccurate.

### 2.2.6 Modified Andreasen and Andersen Model

This model is based on a continuous approach rather than a discrete approach described in all the aforementioned models. The model that was modified by Funk and Dinger (Mangulkar, 2013) can be represented by the following equation:

$$P_t = \frac{d^q - d_{min}^q}{d_{max}^q - d_{min}^q} \quad (2.9)$$

Where  $P_t$  is the fraction of total solids being smaller than  $d$ ,  $d_{max}$  indicates the maximum sieve size (100% passing),  $d_{min}$  is the minimum size of the particle, and  $q$  is the distribution modulus. Since fine particles are not able to pack in the manner that coarse

particles (same in shape) do, Andreasen and Andersen limited the distribution modulus to a range 0.33-0.50 (Wang et al. 2014). The main limitation of this model is that it is based only on particle size distribution, and does not account for aggregate shape and texture.

## 2.3 Empirical gradation optimization methods

While some particle packing methods are based on theory and scientific explanations, other methods are based on the strategy of proportioning particles by trial and error. These empirical methods provide a criterion of “ideal” packing and suggest proportioning particles when attempting to meet given criteria.

### 2.3.1 0.45 power chart

The 0.45 power chart was developed by the concrete industry in 1907, which is a graph of percent passing versus sieve size raised to the power of 0.45. According to this method, the optimum grading is defined by a straight line from the origin to the nominal maximum size of aggregate (Figure 2.4). However, according to the study results of Taylor et al. (2015), aggregate combinations obtained from the 0.45 power chart did not always provide the lowest void content. Ley et al. (2012) also found in their research that the 0.45 power chart is not the best way to obtain aggregate combination for a slip-formed concrete pavement mixture. However, according to Cook et al. (2016), this method can be useful in predicting a water reducer (WR) dosage that was required to pass the Box Test. The closer a combined aggregate curve to the optimum one, the less amount of WR is required. Ramakrishnan (2004) stated that the mixes obtained using the 0.45 power chart resulted in higher strength and better workability compared to such methods as the Shilstone Chart, and the 8-18 curve.

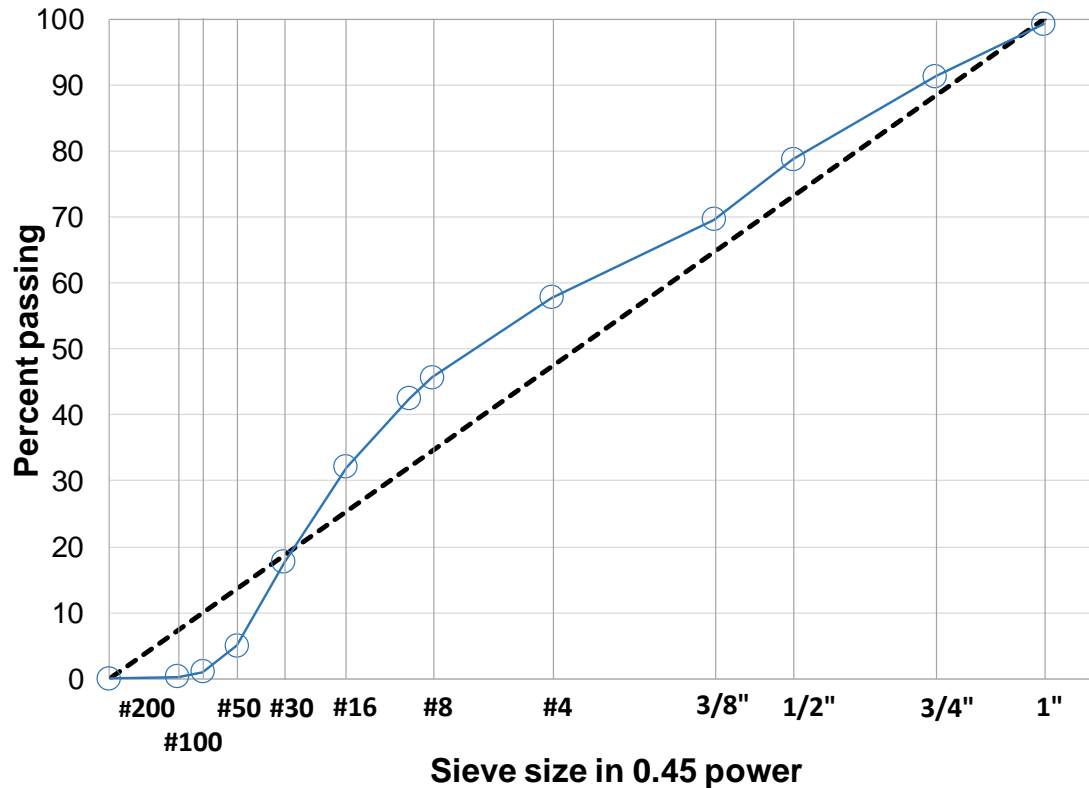


**Figure 2.4. 0.45 power chart**

### 2.3.2 8-18 curve

The 8-18 Chart is a tool based on an individual percent retained (IPR) to provide a uniform blend by limiting the amount of each sieve size particles. It focuses on graphically evaluating excess and deficiency of particles of particular sieve size. Traditionally “8-18” boundaries (Figure 2.5) are suggested for each sieve size from 1/2 in. to #30. According to Cook et al. (2016), it is a useful tool in predicting required WR dosage to achieve appropriate workability. However, Quiroga et al. (2004) stated that “8-18” boundaries do not guarantee good workability, and sometimes low packing cannot be achieved due to lack or excess of either small or large particles, which is why this method should not be used when dealing with aggregates with a high amount of microfines.

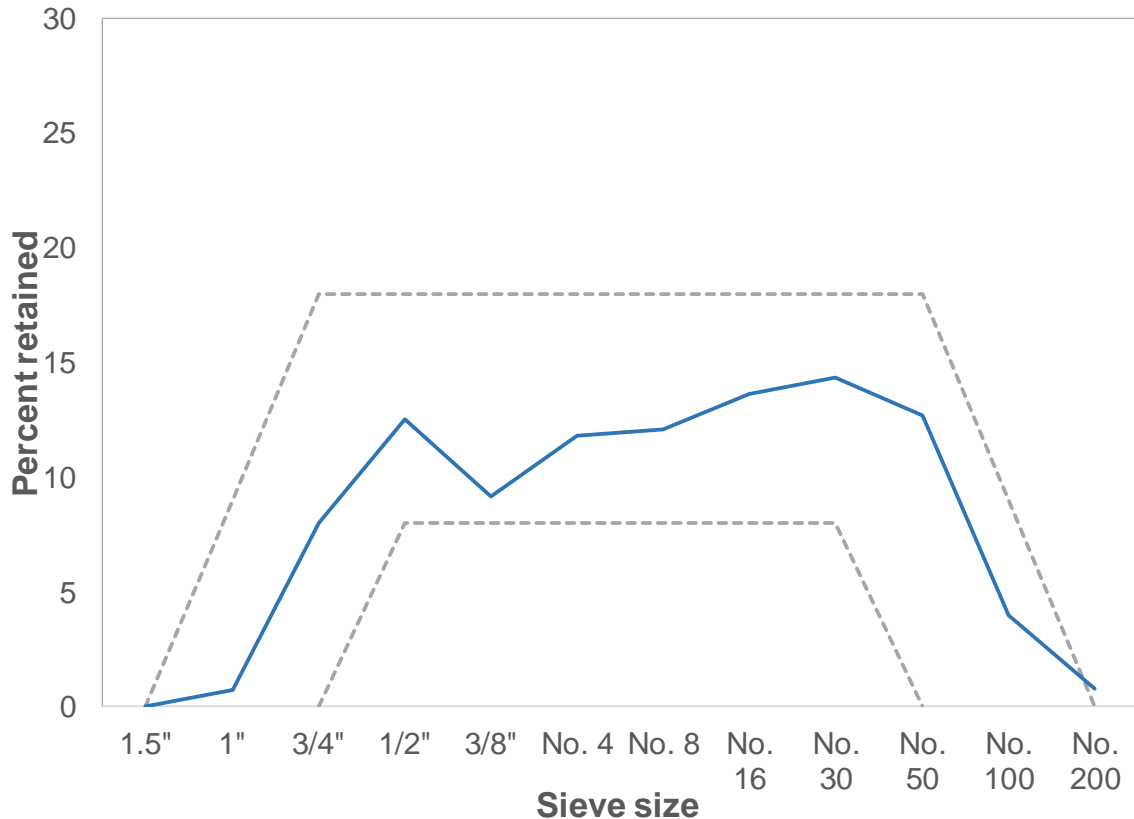


**Figure 2.5. IPR chart with '8-18' limits**

### 2.3.3 Tarantula curve

The Tarantula Curve is an empirical method to proportion aggregate content developed by Ley (2012) after comparing workability of the mixtures with different gradations using the Box Test. Consequently, boundary limits on an individual percent retained chart were modified (Figure 2.6). There are also recommendations for the amount of coarse sand to provide appropriate cohesion (total volume retained on #8 to #30 sieves must be at least 15%), and for the amount of fine sand to provide adequate workability (total volume retained on #30 to #200 must be within 24% and 34%). Historical data from the Minnesota Department of Transportation shows that with time aggregate combinations were developed by trial and error to fall into Tarantula limits

without knowing of the Tarantula Curve (Ley, 2013). According to Taylor (2015), similar results were reported in Iowa, North Dakota, and South Africa. Moreover, Texas slip-formed pavement sections utilizing this method to obtain the mixture showed a good response to vibration and resulted in low cementitious material content (4.75 sacks). This method cannot be used for roller-compacted concrete, self-consolidating concrete, and pervious concrete since the scope of the work focused on slip formed pavement concrete and traditional flowable concrete applications. However, the main issue of this approach is that, though it can define if a blend is good or bad (within Tarantula limits or not), it is not suitable for comparing good blends, i.e. if several blends are within the provided limits, it is hard to tell which one is exactly the optimum one.

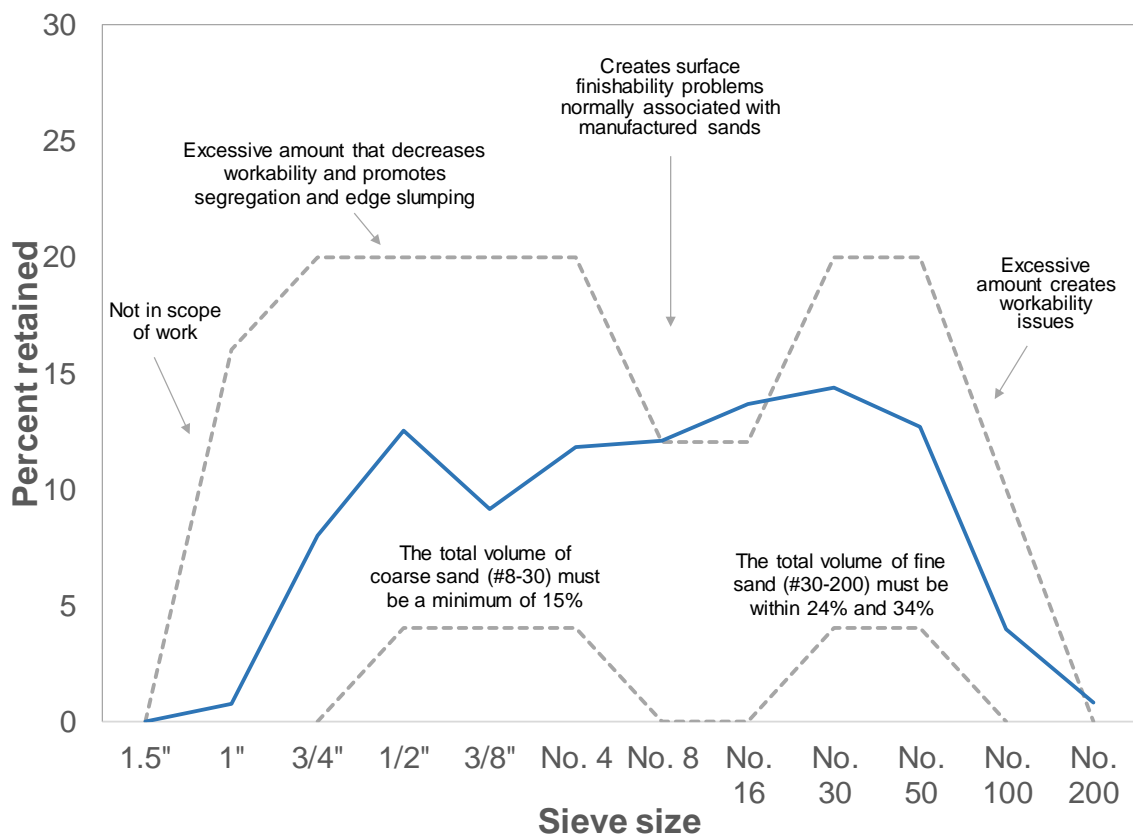


**Figure 2.6. Tarantula curve**

### 2.3.4 Coarseness factor chart

The Coarseness Factor Chart, also called a Shilstone Chart, is a graphical method to analyze combined aggregate particle distribution. The chart is made up of a coarseness factor (CF) as a horizontal axis and a workability factor (WF) as a vertical axis. CF and WF can be calculated using equations (2.10) and (2.11). The chart is divided into five different zones (Figure 2.7). Zone I stands for the gap-graded mixtures. Due to deficiency of intermediate aggregates, there is a high risk of segregation during consolidation. Zone II indicates a well-graded mixture with a maximum aggregate size from 1.5 in. to  $\frac{3}{4}$  in. Zone III is a continuation of Zone II but with a maximum aggregate size equal or smaller than  $\frac{1}{2}$  in. Zone IV represents mixtures with an excess of fine particles, which can lead to segregation and high permeability. Mixtures falling to Zone V have an excess of coarse particles.

$$WF = W + \left( 2.5 * \frac{C-564}{94} \right) \quad (2.10)$$

Where, W is the cumulative percent passing No.8 sieve, and C is the cementitious material content (lb/yd<sup>3</sup>).

$$CF = \left( \frac{Q}{R} \right) * 100 \quad (2.11)$$

Where, Q is the cumulative percent retained on the 3/8 sieve, and R is the cumulative percent retained on the No.8 sieve.

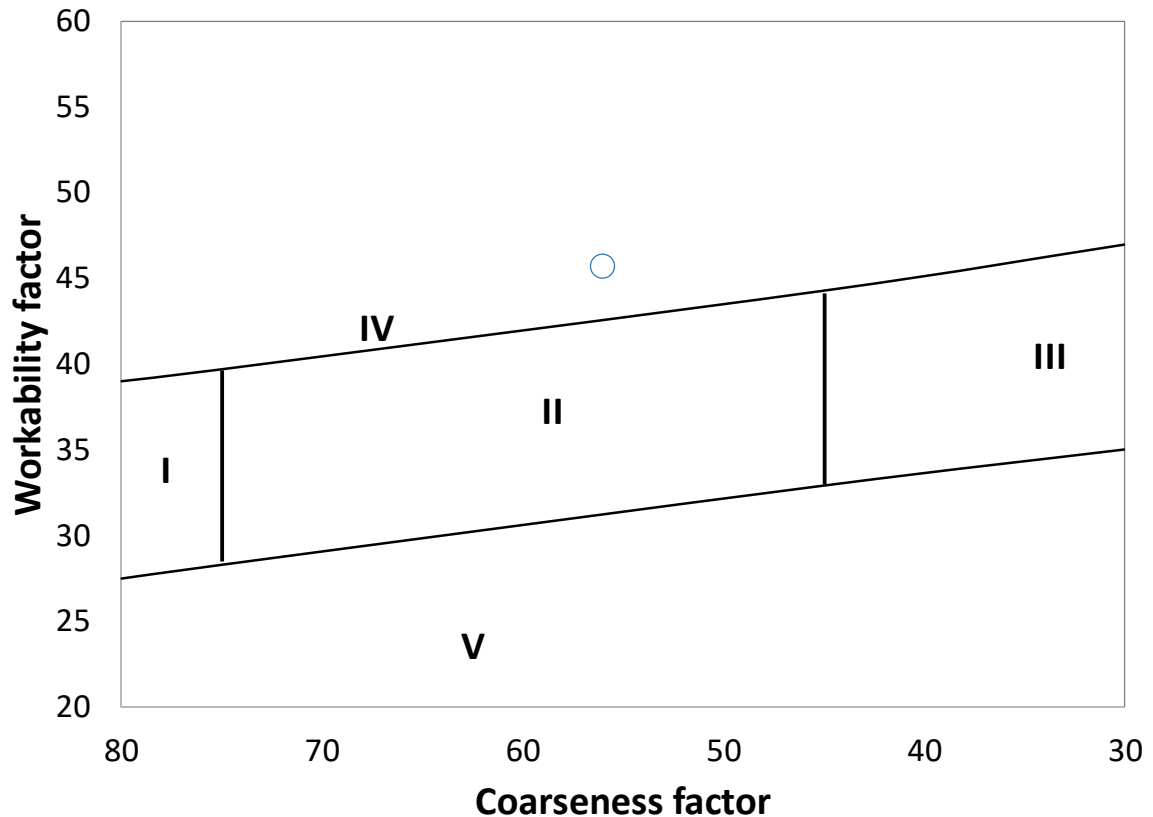


**Figure 2.7. Coarseness factor chart**

According to Ley et al. (2012), the location on a Coarseness Factor Chart does not necessarily have a significant relationship to the response of a concrete mixture to vibration. However, it was found that mixes falling into Zone II were able to hold an edge. Cook et al. (2016) concluded that the coarseness factor is not a useful tool to predict the water reducer dosage required for adequate workability of pavement concrete. A single location on the chart did not result in similar WR demand. Conversely, some mixtures were located at different regions but resulted in almost the same WR dosage to pass the Box Test. According to Obla (2007), optimizing aggregate gradation using a Shilstone Chart does not result in a lower void content within the aggregate matrix.



## 2.4 Factors impact aggregate packing and workability of pavement concrete

### 2.4.1 Maximum size of aggregate

A larger maximum size of aggregate is reported to positively impact concrete workability due to less specific surface area of aggregate (Quiroga et al., 2004). In an investigation of optimized graded concrete, Cook et al. (2013) examined the influence of the maximum size of aggregate by analyzing mixtures with three different maximum sizes with the same sand content and no particles of one sieve size exceeding 20%. Larger aggregate size resulted in lower WR dosage necessary to pass the box test, but the difference is too insignificant to state that increasing maximum size can lead to better workability. It was also mentioned that using larger aggregate size could be beneficial in producing aggregate gradation with no excessive content of material on a single sieve size because there would be more sizes to distribute aggregate. Ley (2012) attempted to correlate results from the slump test and box test. It was found that, due to the stronger aggregate interlocking, mixes with coarse aggregate with a maximum size of 1.5 in. required a higher slump to pass the box test compared to  $\frac{3}{4}$  in. coarse aggregate.

### 2.4.2 Gradation

It is useful to analyze the combined aggregate grading as they present in a concrete mixture. Sometimes there is a deficiency of mid-sized aggregate (around 3/8 in), which leads to concrete with high shrinkage properties, poor workability, and high water demand (Kosmatka et al. 2008). Kosmatka et al. (2008) referred to Abrams (1918) and Shilstone (1990) who mentioned benefits of combined aggregate analysis: by keeping cement content constant, the optimum aggregate combination can be found that will lead

to the most effective water to cement ratio and higher strength. In addition to this, mixtures with optimum gradation respond best to a high-frequency vibrator.

### 2.4.3 Aggregate shape and texture

The aggregate shape is a very important characteristic that has an impact on paste demand, workability, and strength. According to Kosmatka et al. (2008), aggregate shape and texture have more impact on fresh concrete rather than hardened concrete. The shape is mainly associated with sphericity, flatness, angularity, and roundness (Quiroga et al. 2004). The aggregate texture is mainly related to roughness of a particle. Rached et al. (2009) found that mixtures with poor aggregate shape required more cement paste. Cook et al. (2016) concluded that angularity and number of flat particles play a significant role in workability of pavement concrete. Based on Quiroga (2004), a high amount of flat coarse aggregates can lead to finishability issues. Aggregate shape and texture significantly influences particle packing. Kwan (2002) compared the correlation between different aggregate shape characteristics (flakiness ratio, elongation ratio, sphericity, shape factor, convexity ratio, and fullness ratio) and particle packing. Results indicated that the two factors most affecting the particle packing are shape and convexity factors. They had a correlation coefficient of 0.859 and 0.828, respectively, when considered as individual factors; when considered together, the correlation coefficient was 0.893. Obla (2011) and Quiroga et al. (2004) stated that concrete workability is affected by the shape and texture of fine aggregate more than coarse aggregate.

### 2.4.4 Microfines content

Aggregate particles finer than 75 microns (#200 sieve), usually referred to as silt or clay, can be present in sand and gravel deposits (Lamond et al., 2006). It can also be

present as dust from crushing and mechanical processing. Typically, the higher the amount of microfines, the greater the necessity for an increased water demand and reduced air content (Obla, 2011).

## 2.5 Mixture design development

There are several mixture design procedures reported for pavement concrete developed by research groups from the University of Texas-Austin and the National Concrete Pavement Technology Center. Siddiqui et al. (2014) proposed a mix design method for pavement concrete, where the optimum aggregate blend is selected based on the 0.45 power chart. Once the optimum blend is obtained, a combined aggregate void content test is used to determine how much paste is to be added. This design procedure suggests designing concrete so that the paste volume equals the void content of the combined aggregate blend and then adjusting it further after trial batches. However, it is well known that excess paste is required to provide adequate workability. Therefore, the design procedure seems to have unnecessary steps of trial mixes without an excess paste. Also, as it was mentioned before, the 0.45 power chart does not always provide the optimum blend because it does not take into consideration aggregate shape and texture. A mix design procedure proposed by Tylor et al. (2015) is based on a similar technique as described in Siddiqui et al. (2014). In addition to the 0.45 power chart, the Tarantula Curve is used to optimize aggregate gradation. Once the void content of the combined aggregate is obtained experimentally, the volume of paste over the volume of voids ratio ( $V_{\text{paste}}/V_{\text{voids}}$ ) was the main driving criteria. The recommended initial  $V_{\text{paste}}/V_{\text{voids}}$  is 1.25-1.75. Besides the slump test, the VKelly Test was used to evaluate the behavior of fresh concrete under vibration.

## 2.6 Quality control tests

ASTM C29 (Standard Test Method for Bulk Density (Unit Weight) and Voids in Aggregate) is a test used to determine bulk density and void content of aggregate in the compacted or loose condition. Standard compaction methods included in the standard test are rodding, jiggling, and shoveling. However, the test is limited to one aggregate only. According to Kosmatka (2008), it is important to analyze the combined aggregate gradation as it is more representative of the configuration present in a concrete mixture. Therefore, the test was modified to determine the void content of the combined aggregate matrix. The combined void content test is a tailored adoption of the test procedure as described in ASTM C29 that was developed to measure the particle packing density and void content with the incorporation of multiple aggregates at different proportions (Obla, 2007). Moreover, it is believed that introducing vibration with a pressure compaction method is appropriate. This method results in a higher compaction factor, and it is more representative of pavement applications as pavement concrete is generally vibrated during placing.

It is important to justify the optimum blends based on fresh concrete performance. Both studies discussed in the previous subchapter lacked a more appropriate analysis of fresh concrete properties to justify pavement concrete performance. For slip-forming paving, it is necessary for concrete to be consolidated under vibration, but also to be able to hold an edge after vibration is stopped and formwork is removed. The slump test is not sufficiently sensitive in evaluating low workability mixtures for slip-forming applications. Therefore, it is necessary to conduct additional tests to better understand the fresh properties of pavement mixtures. The Box Test was developed to examine the

response of fresh concrete under vibration, which can be assessed by the amount of surface voids observed on the sides and the appearance of edge slump (Cook et al., 2014).

As the Box test is largely subjective in the surface evaluation, another test – the VKelly test – is a quantitative test that can be applied. The VKelly Test is the modified test from the standard test method for ball penetration in freshly mixed hydraulic cement concrete (ASTM C360) and was developed by Taylor et al. (2012). The main purpose of the test is to observe the dynamic behavior of pavement concrete under vibrations by evaluating the penetration depth of a vibrating ball over time.

## 2.7 NDOT historical data

Figures 2.8, 2.9, 2.10 illustrate some documented blends used in pavement mixes in Nebraska that were obtained from Heyen et al. (2013) and Nebraska Department of Transportation (NDOT) internal reports. From Figures 2.8 and 2.9, it can be noticed that the blends used in Nebraska have a significant excess in No. 8 and No. 16 sieve sizes, and a lack of 3/4 in. and 3/8 in. size particles. Figure 2.10 also demonstrates that the majority of the blends with standard cement content used are out of recommended zones. While it is fair to state that gradations used in Nebraska pavement concrete are far from the optimum packing, it is difficult to determine which gradation will work better due to the unique type and gradation of aggregate being used.

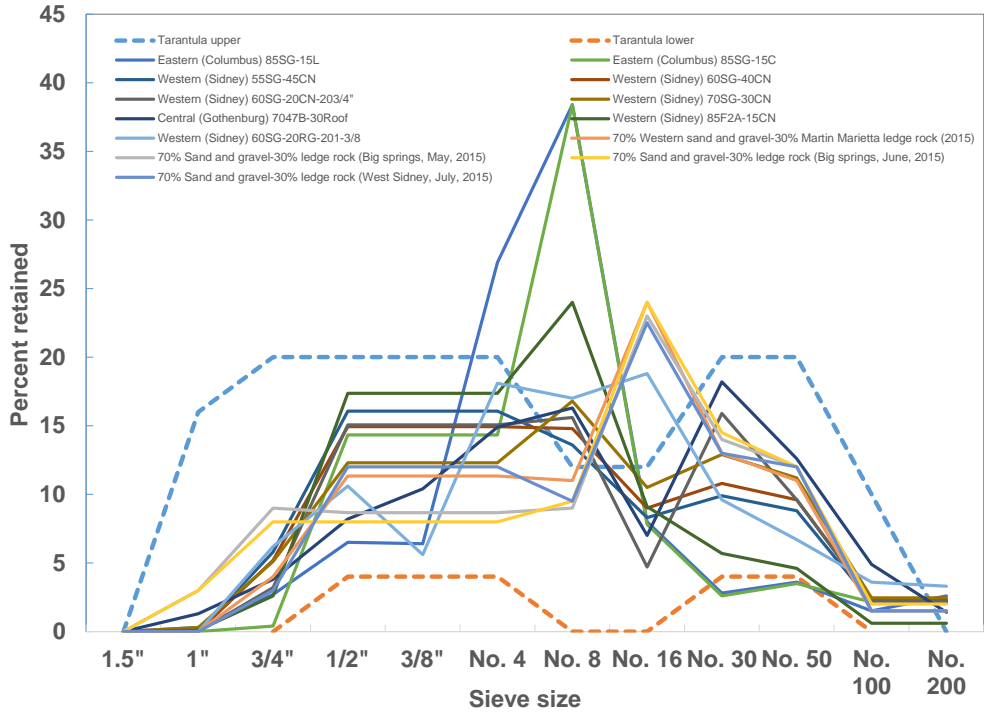


**Figure 2.8. Nebraska gradations on Tarantula curve**

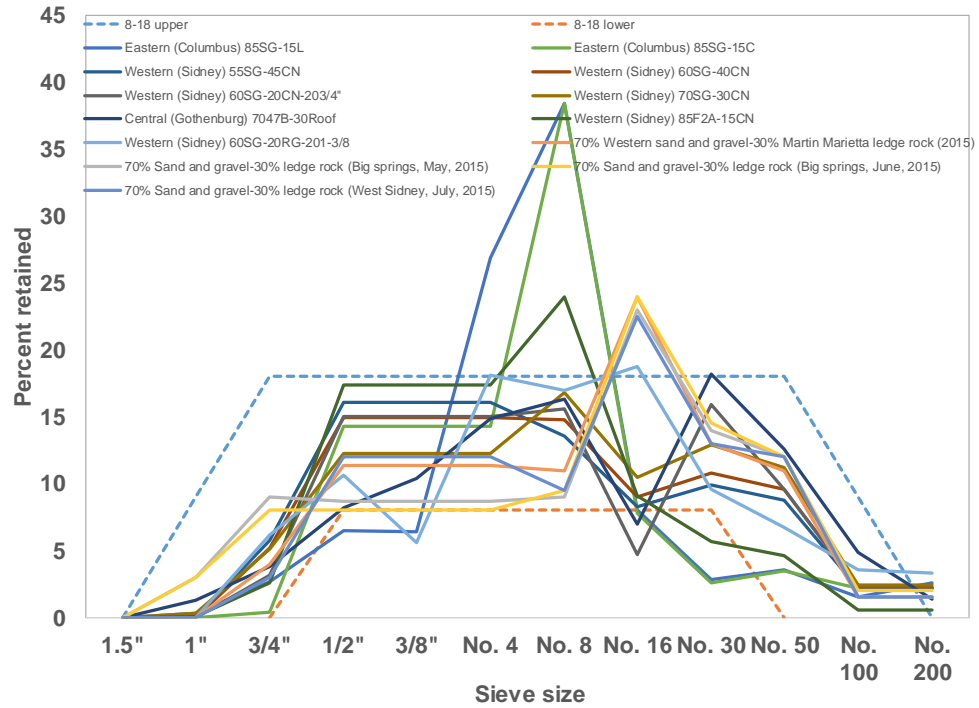


**Figure 2.9. Nebraska gradations on 8-18 curve**

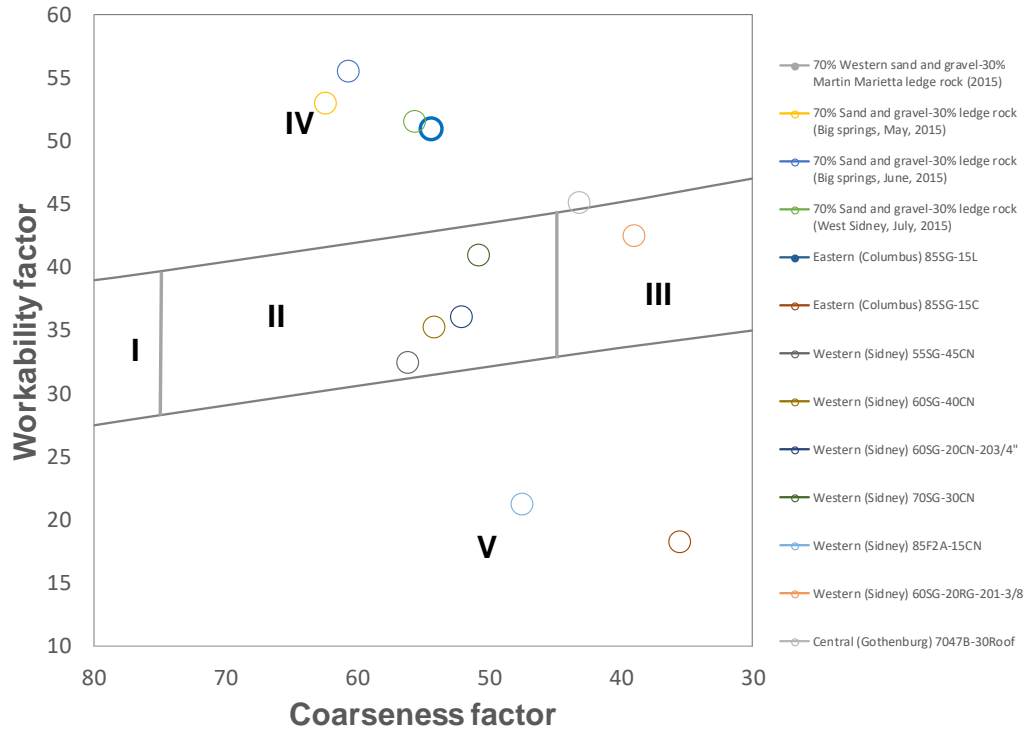


**Figure 2.10. Nebraska gradations on Shilstone chart**

## 2.8 Summary

Based on the literature review conducted, it was determined that proceeding with a discrete theoretical model was the best option. Even though there is slightly more experimental work required to obtain necessary inputs, there are a few advantages over empirical optimization methods. The first advantage is that the approach includes the consideration of aggregate shape and texture, although they are accounted for indirectly. Another advantage of discrete theoretical models is that they can quantitatively predict the packing degree, whereas the empirical models are only capable of comparing aggregate blends. Among the presented models, the Modified Toufar Model was selected due to its accurate correlation with experimental results and relative simplicity compared to such complex models as the LPDM or the CPM.

Various factors impacting aggregate packing and pavement concrete workability were discussed. It was found that the aggregate gradation, shape, and texture are the driving criteria in aggregate packing. It is believed that the shape and texture of fine aggregate plays a more important role compared to coarse aggregate. Besides these two parameters, the maximum size of aggregate and microfines content are critical in fresh concrete performance.

Different mixture design procedures developed by other researchers were reviewed. It was found that even though the philosophy is reasonable, there is a lack of fresh pavement concrete performance analyses. In addition, methods used to optimize aggregate gradation in these studies do not account for aggregate shape and texture.

In terms of quality control tests, it was decided to proceed with the combined void content test with an additional compacting method, which is vibration plus pressure. Performance of fresh pavement concrete can be justified with the help of special tests such as the Box and VKelly tests. Both of them will be used further and analyzed for their effectiveness.

Finally, gradations of different aggregate blends that are being used in Nebraska were obtained from the previous research project reports and NDOT internal reports. Since only gradation information was available, it was only practical to analyze blends based on empirical methods. The Shilstone Chart, 8-18 Curve, and Tarantula Curve have shown that the currently used aggregate blends are far from optimum.



## CHAPTER 3. EXPERIMENTAL PROGRAM

### 3.1 Introduction

It was critical to select representative materials for Nebraska for efficient research. This chapter presents the materials (cementitious materials, aggregates, and chemical admixtures) selected for this study including necessary properties and the justification for their selection. The main materials used in this study were as follows: IP cement with 25% blended class F fly ash as the main cementitious material; limestone, granite, and two types of sand and gravel as representative aggregates; air-entraining agent and mid-range water reducer as chemical admixtures.

Test methods with corresponding standards to evaluate concrete behavior in the fresh state, hardened state, and in the long-term are also presented. Besides standard tests including slump and setting time, fresh concrete behavior was characterized by special pavement workability tests such as the Box and VKelly tests, which are also presented in this chapter. To examine hardened concrete properties, compressive strength, flexural strength, and modulus of elasticity tests were used. Moreover, test procedures such as freeze/thaw resistance, surface and bulk resistivity, free shrinkage, and restrained shrinkage, which were used to observe long-term durability behavior, are also presented.

### 3.2 Materials

#### 3.2.1 Cement and cementitious materials

NDOT Standard Specifications for Highway Construction (2017) require the use of IP interground/blended cement for pavement application. IP cement was designed to mitigate Alkali-Silica Reaction (ASR), provide sulfate resistance, and reduced chloride

permeability. For this study, type IP Portland-pozzolan cement with 25% blended class F fly ash content that meets ASTM C595 (Standard Specification for Blended Hydraulic Cements) was used as the cementitious material. The chemical composition and physical properties of cement used in the study are reported in Table 3.1.

**Table 3.1. Chemical composition and physical properties of IP cement**

Chemical Properties	Pozzolan content, %	25
	MgO, %	2.45
	SO <sub>3</sub> , %	3.10
	Loss in Ignition, %	1.00
Physical Properties	Blaine Fineness, cm <sup>2</sup> /g	4400
	Specific Gravity	2.95

### 3.2.2 Aggregates

In order to evaluate the effectiveness of the aggregate gradation optimization, aggregates from different locations were collected and used in the present study. From East NE, combined sand and gravel (SG) and 1 in. nominal maximum size aggregate of limestone (LS) were used, which are the most commonly used aggregates for pavement concrete in East NE. In order to select aggregates from West and Central NE, gradations from different aggregate sources were collected and analyzed. Figure 3.1 represents gradations of representative West and Central NE aggregates. It was noted that aggregates from Central NE identified in this study are very similar to the aggregates from East NE. Therefore, it was decided to only incorporate East NE and West NE aggregates in this study. In West NE, usage of sand and gravel, limestone, and granite is predominant. In general, sand and gravel in West NE is coarser. However, limestone and granite aggregates are finer than East NE limestone.

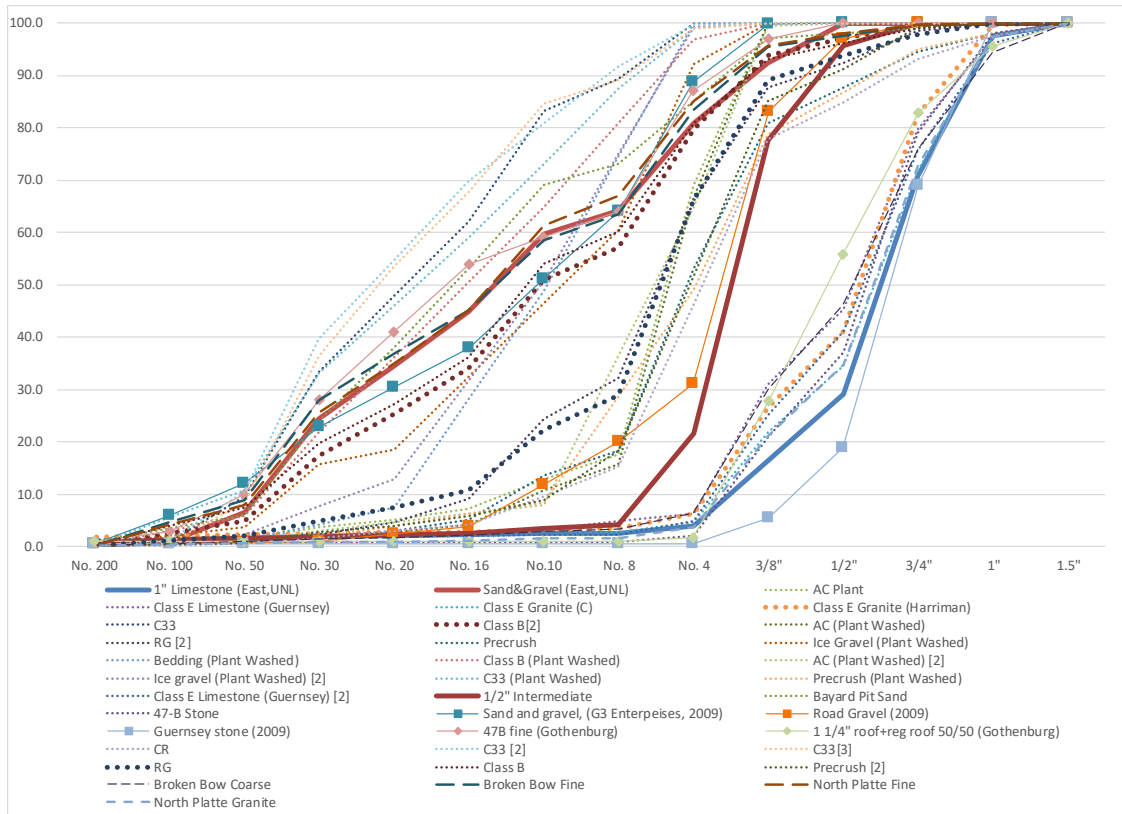


**Figure 3.1. Nebraska aggregates gradations**

In order to test aggregates and concrete as different from East NE as possible, combined sand and gravel (SG\_W) with the highest fineness modulus, and 1 in. nominal maximum size granite (GR) with the lowest fineness modulus were selected from West NE. Selected aggregates can be seen on Figure 3.2.



**a) 1" Limestone**



**b) Sand and gravel (East NE)**



**c) 1" Granite**



**d) Sand and gravel (West NE)**

**Figure 3.2. Selected aggregates**

Figure 3.3 presents the particle size distribution of aggregates based on sieving analysis performed according to ASTM C136 (Standard Test Method for Sieve Analysis of Fine and Coarse Aggregates). The specific gravity at saturated surface dried (SSD) condition, and the absorption of coarse and fine aggregates were obtained in accordance with ASTM C127 (Standard Test Method for Relative Density (Specific Gravity) and Absorption of Coarse Aggregate) and ASTM C128 (Standard Test Method for Relative

Density (Specific Gravity) and Absorption of Fine Aggregate), respectively. The obtained values along with the fineness modulus (FM) are presented in Table 3.2.

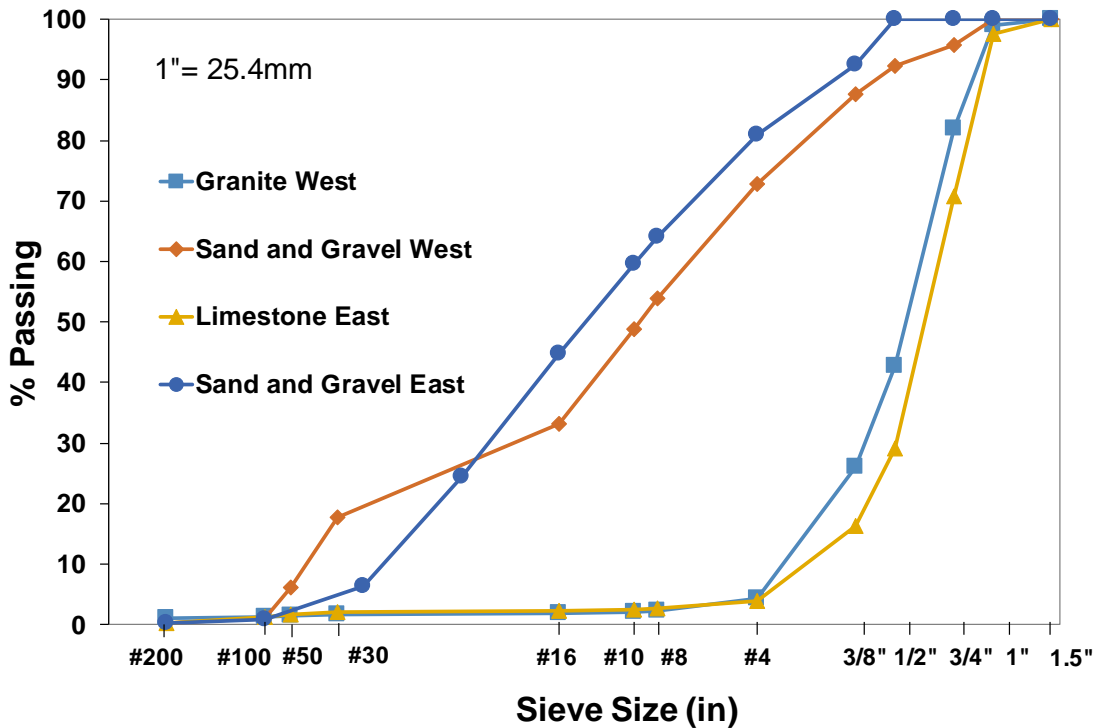


Figure 3.3. Gradation curve of aggregates used in this curve

Table 3.2. Aggregates properties

Properties	SG	LS	SG_W	GR
Specific gravity	2.586	2.671	2.567	2.652
Absorption (%)	0.96	0.91	1.35	0.70
Fineness modulus	3.86	6.99	4.32	6.79

### 3.2.3 Chemical admixtures

MasterAir AE90 for East NE mixes and AE200 for West NE and performance evaluation mixes were used as the air entraining agents. These admixtures meet ASTM C260 (Standard Specification for Air-Entraining Admixtures for Concrete). Eucon X-15

that meets ASTM C494 (Standard Specification for Chemical Admixtures for Concrete) was used as a mid-range water reducer (WR).

### 3.3 Combined aggregate void content test

To obtain the amount of excess paste in each specific mix, a combined void content test was conducted. The test is a tailored adoption of the test procedure as described in ASTM C29, which was developed to measure the particle packing density and void content with the incorporation of multiple aggregates at different proportions (Obla, 2007). Figure 3.4 is an example of the mixed aggregates (3.4a) and representative aggregate combination demonstrating different packing degrees (3.4b). To ensure proper mixing, aggregates were mixed in a 1.7 ft<sup>3</sup> (0.0481 m<sup>3</sup>) capacity drum mixer for one minute followed by hand mixing for another minute. In addition to the three standard compaction methods, i.e., shoveling, rodding, and jiggling procedures, a vibration plus pressure method as suggested by De Larrard (1999) was used for the void content measurement. The fourth method results in a higher compaction factor, and it is more representative for pavement application as pavement concrete is generally vibrated during placing. In this method, a steel container of a volume of 0.25 ft<sup>3</sup> (0.0071 m<sup>3</sup>) and filled with aggregates was placed on a vibration table with a 1.45 psi (10 kPa) applied external pressure on top. It was simultaneously vibrated at a medium amplitude for one minute (see Figure 3.5). The specific gravity of the blended fiber-aggregate mixture was calculated as:

$$G_{sb,combined} = \frac{1}{\frac{P_{LS}}{G_{sb,LS}} + \frac{P_{SG}}{G_{sb,SG}}} \quad (3.1)$$

Where  $G_{sb}$  and  $P$  represent the specific gravity and fraction of each component.

The bulk density of the combined mixture can be calculated as:

$$\text{Bulk Density} = \frac{\text{Mass}}{\text{Volume}} \quad (3.2)$$

Where Mass is the total mass of material in the measure, and Volume is the volume of the measure.

The void content (% Void) of the mixture was calculated as:

$$\% \text{Void} = \frac{G_{sb,combined} \times UW_{water} - \text{Bulk Density}}{G_{sb,combined} \times UW_{water}} \quad (3.3)$$

Where  $UW_{water}$  is the unit weight of water.

The void content of each aggregate combination was measured three times and the average value was reported.



**a) Test setup**



**b) Visual examination of aggregate packing with different combinations**

**Figure 3.4. Combined void content test**

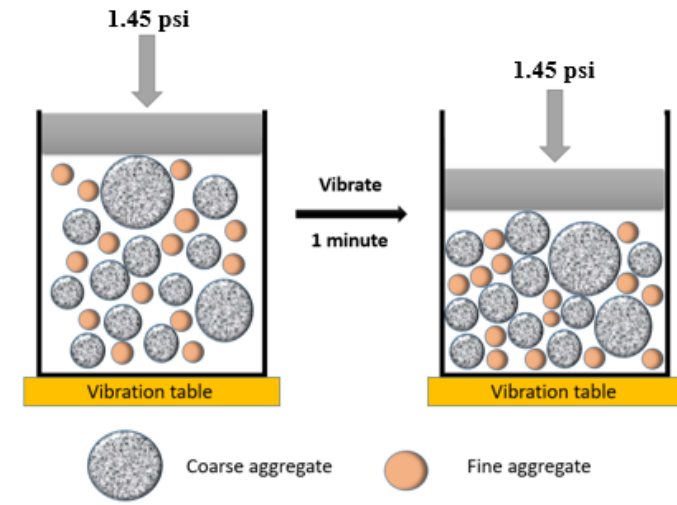


**Figure 3.5. Vibration plus pressure method sketch**

### 3.4 Concrete mixing

A drum mixer with a 3 ft<sup>3</sup> (0.0849 m<sup>3</sup>) capacity was used to mix concrete following the procedure described in ASTM C192 (Standard Practice for Making and Curing Test Specimens in the Laboratory). First, coarse aggregate was mixed with approximately half of the mixing water containing AEA for 30 seconds. Then, sand and gravel, cement, and the remaining water were added and mixed for 3 minutes, followed by a 3 minute resting period, and ending with a 2 minutes mixing period. If it was necessary to adjust workability, WR was added and concrete was mixed for an additional 3 minutes. In the performance evaluation phase, when WR dosage was already known for a particular mixture, it was added with the second half of the water. Prior to mixing, aggregates were brought to saturated condition and the water amount was adjusted accordingly prior to the batching of each mix, which was 1.3 ft<sup>3</sup> (0.0368 m<sup>3</sup>) in size.



### 3.5 Fresh concrete tests

#### 3.5.1 Slump test

A concrete slump was measured according to ASTM C143 (Standard Test Method for Slump of Hydraulic-Cement Concrete) to measure the consistency of concrete (Figure 3.6). The test was performed immediately after the concrete mixing was completed.



**Figure 3.6. Slump test setup**

#### 3.5.2 Air content test

Air content of the mixtures was measured according to ASTM C231 (Standard Test Method for Air Content of Freshly Mixed Concrete by the Pressure Method) using a type B meter (Figure 3.7).



**Figure 3.7. Air pressure meter**

### 3.5.3 Setting time test

Concrete setting time was tested in accordance with ASTM C403 (Standard Test Method for Time of Setting of Concrete Mixtures by Penetration Resistance). Once mixing is completed, coarse aggregates were sieved out from the concrete, and mortar was tested for setting time (Figure 3.8).



**Figure 3.8. Setting time test setup**

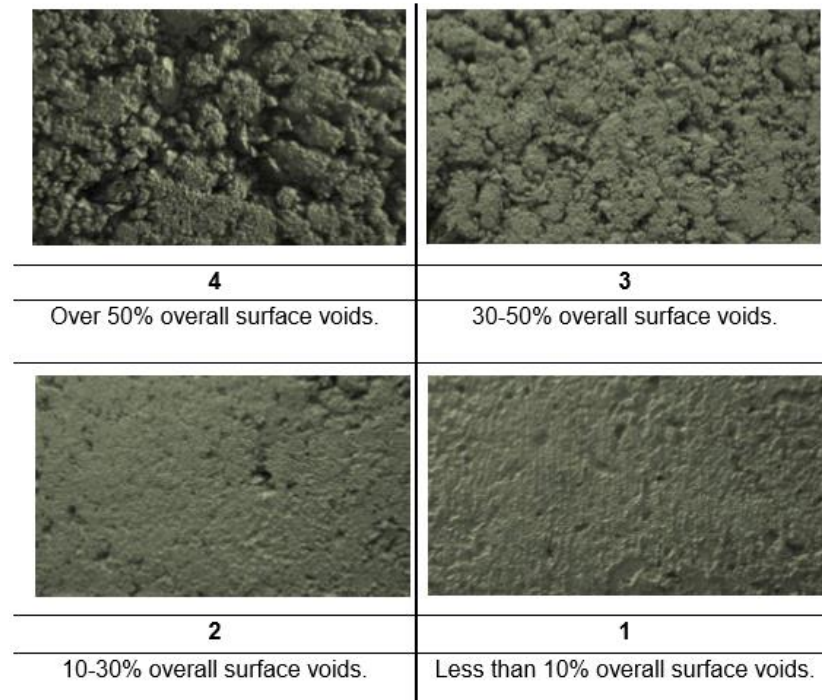
#### 3.5.4 Box Test

For the Box Test, fresh concrete was loosely placed into a temporarily fixed wooden box with an open top and bottom and a dimension of 1ft×1ft×1ft (0.3m×0.3m×0.3m) (Figure 3.9). A portable electrical vibrator was then used to consolidate the concrete for 6 seconds. A vibrator was inserted vertically at the center of the specimen to full depth for 3 seconds, and then raised for 3 seconds. The wooden box was then removed sideways and the surface was visually examined for surface voids and a straight edge is used to exam edge slumping. While a visual examination of the surface void content is commonly used, in order to have a more objective measurement, a commercial image process software named ImageJ was used to obtain the exact value of surface voids using photos of the four sides taken after the removal of sides. As shown in Figure 3.10a, the original method determined the visual ranking largely based on roughly estimating the amount of surface voids. Even with the recent attempt to improve the

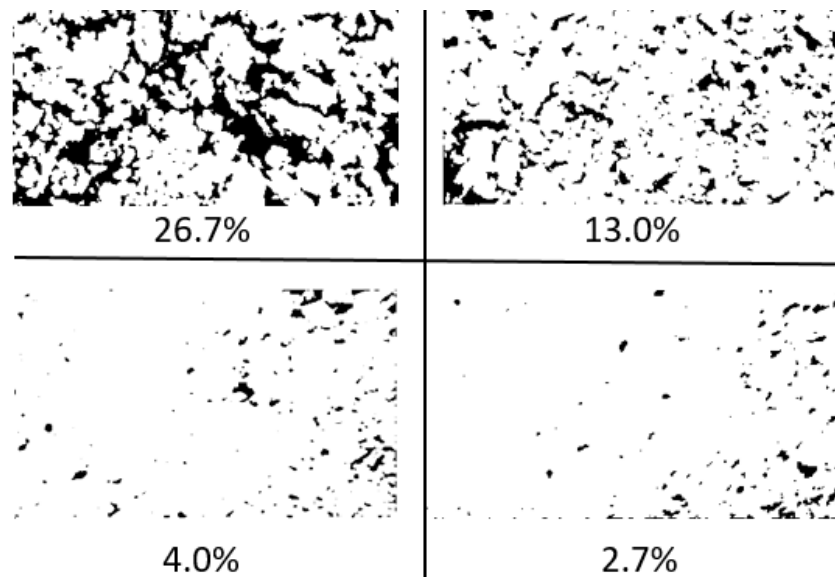
accuracy with a procedure to place a piece of transparent paper with dots on the concrete surface to count the voids, the measurement is still relatively subjective. The new methods use the image software to calculate the percentage of voids on all four sides, which largely eliminates the human factor. Figure 3.10 illustrates the difference in surface void evaluations based on the original method and based on the imaging software method used in the current study. The example, as illustrated in Figure 3.10b, demonstrates that the image software can clearly identify surface voids. Note that the new method resulted in a lower amount of voids identified compared to the original method. According to the comparison of voids based on the original visual measurement and the image software from the Box Tests with over thirty difference mixes, a revised ranking system based on the software calculated surface voids was determined. The new ranking range using the image analysis method was designed as follows: 0-3% classified as ranking 1, 3-5% as 2, 5-15% as 3, and over 15% as 4.



**Figure 3.9. Box test setup**



(a) Surface voids from Cook et al. (2016)



(b) Surface voids from image process

Figure 3.10. Comparison of surface voids of box test rankings from different methods

In terms of the edge holding ability, standard procedure presents a basic pass/fail evaluation according to edge slump by classifying a mix as failed if the deflection is more than 1/4". However, even if the mixture passes, the holding edge quality might differ. Therefore, it was decided to modify the rating based on smoothness of edges. The idea was borrowed from the old measurement of Floor Flatness ( $F_F$ ) number, where the greatest defect along a specified length was measured. The edge quality ranking was modified as follows and is based on the greatest defect along edges: 1-good (<1/16 in), 2-average (1/16-1/8 in), 3-poor (1/8-1/4 in), 4-failed (>1/4 in) (Figure 3.11). If it failed because of a notable lack of paste, ranking 4a was assigned; if a failure is due to an abundance of excess of paste, ranking 4b was assigned. Finally, a dual index was used to describe Box Test performance with "E" standing for edge quality and "S" for surface quality. For example, "E2-S1" stands for a mixture with an average edge quality and ranking 1 in terms of surface voids.



**a) 1-good edge quality**



**b) 2-average edge quality**



**c) 3-poor edge quality**



**d) 4a-failed edge quality**



**e) 4b-failed edge quality (abundance of excess paste)**

**Figure 3.11. Examples of Box test results with different edge holding abilities**

According to the procedure from Cook et al. (2016), if a mixture does not pass the Box Test, WR can be added to improve workability. The mixture was remixed for an additional 3 minutes after the introduction of WR, and fresh concrete tests were repeated

to examine if acceptable workability was achieved. The procedure can be repeated until it passes the 60-minute mark after the completion of the initial mixing or a significant slump loss is observed.

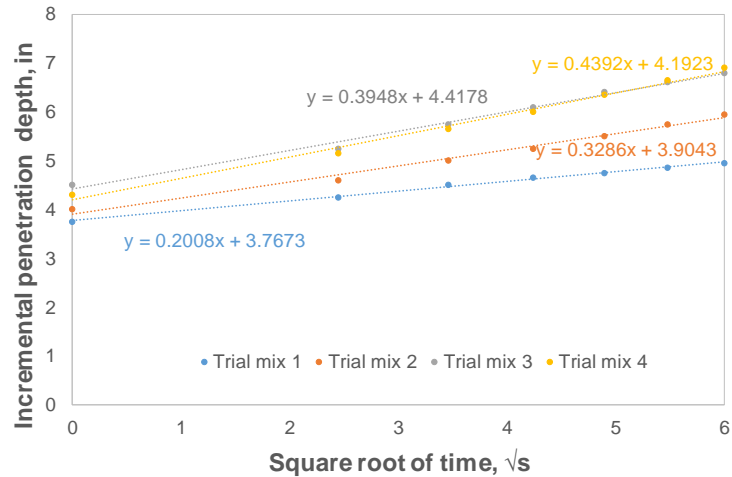
### 3.5.5 VKelly Test

Considering the Box Test is largely subjective (particularly the edge quality portion), the VKelly Test, which is a quantitative test, was adopted in this study. The VKelly Test is a modified test from the standard test method for ball penetration in freshly mixed hydraulic cement concrete (ASTM C360) and was developed by Taylor et al. (2012), as seen in Figure 3.12a. The main purpose of the test is to observe the dynamic behavior of pavement concrete under vibrations by evaluating penetration depth of a vibrating ball against time. The fresh concrete was first placed in a rubber container with a minimum depth of 6 in. The ball was then slowly lowered until it touched the surface and was then released. Vibration was then introduced, and the penetration readings were recorded every 6 seconds during a 36-second period. A graph of penetration depth versus the square root of time was plotted and the slope was obtained as the  $V_{\text{index}}$ . The recommended  $V_{\text{index}}$  range stated by Taylor et al. (2012) is 0.8-1.2. During trial mixes of the study, it was noticed that the standard vibration frequency suggested (8000vpm) is too high due to the higher amount of fine aggregate in the mixture used in this study. As a result, the ball penetrates too fast, which makes it impractical to obtain sufficient points to construct a graph to calculate  $V_{\text{index}}$ . A lower frequency at 5000vpm was therefore used in the study. Examples of the results from VKelly with the current setup are shown in Figure 3.12b.





a) Test setup



b) Examples of results

Figure 3.12. VKelly test

### 3.6 Specimen casting and curing

Upon the completion of mixing, specimens were prepared according to ASTM C192 (Standard Practice for Making and Curing Test Specimens in the Laboratory). All specimens were stored in a 73°F (22.8 °C) room prior to demolding. Demolding was carried out at 24 hours and then stored in a curing room with 100% R.H. and 73°F (22.8 °C) until testing.

### 3.7 Hardened concrete tests

#### 3.7.1 Compressive strength test

Three 4" by 8" cylinders were tested for compressive strength for each mixture based on ASTM C39 (Standard Test Method for Compressive Strength of Cylindrical Concrete Specimens) at 7 and 28 day ages. A Forney compressive machine with a capacity of 400 kips (1,779 kN) was used (see Figure 3.13).



**Figure 3.13. Compressive strength test setup**

### 3.7.2 Flexural strength test

One 6" by 6" by 20" beam was tested for modulus of rupture for each mixture at the age of 28 days according to ASTM C78 (Standard Test Method for Flexural Strength of Concrete (Using Simple Beam with Third-Point Loading)). A Forney beam testing machine with a capacity of 30 kips (133 kN) was used (see Figure 3.14).



### Figure 3.14. Flexural strength test setup

#### 3.7.3 Static modulus of elasticity test

A modulus of elasticity test was performed at 28 days according to ASTM C469 (Standard Test Method for Static Modulus of Elasticity and Poisson's Ratio of Concrete in Compression). A frame with two dial gauges to monitor both axial and radial deformations was used (see Figure 3.15). Each test was recorded and later used to build a graph, from which properties were calculated.



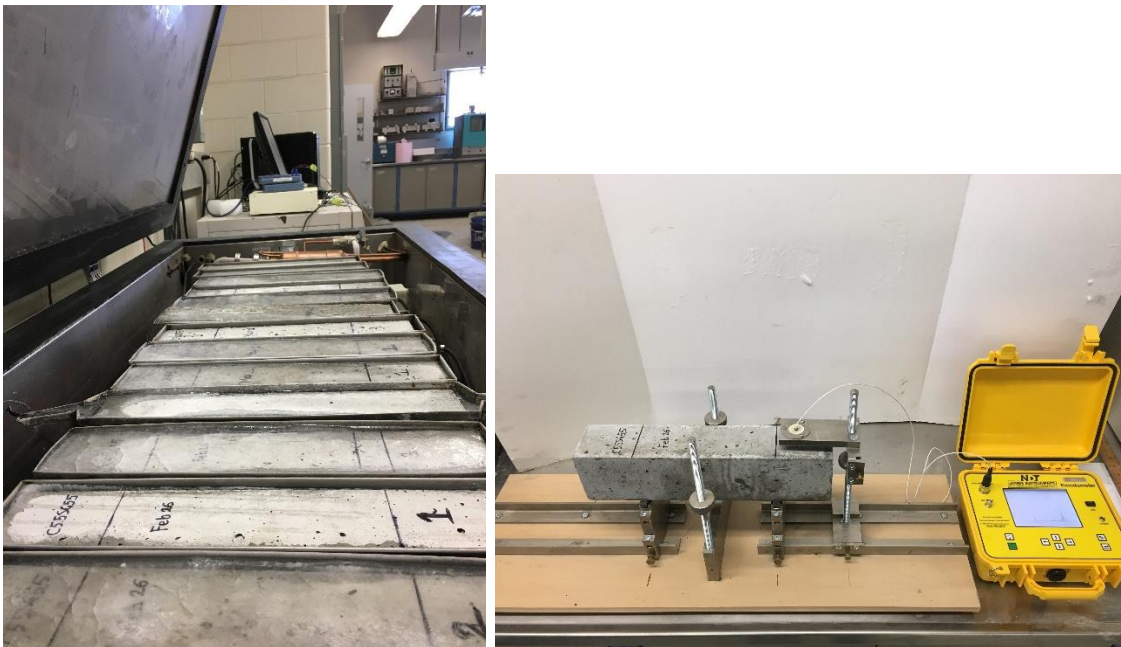
Figure 3.15. Static Modulus of Elasticity test setup

## 3.8 Durability tests

### 3.8.1 Freeze/thaw resistance

The freeze/thaw test was conducted according to ASTM C666 (Standard Test Method for Resistance of Concrete to Rapid Freezing and Thawing) Procedure A. A Humboldt freeze thaw cabinet, which has multiple channels with one being a control, was

used (see Figure 3.16a). Three 3"× 4"× 16" prisms were tested per mixture and the average values were reported. Specimens were exposed to freezing/thawing cycles after 14 days of standard curing. NDT E-meter MK II was used to obtain fundamental transverse frequency approximately every 30 cycles. In addition to this, mass loss was measured. Equipment setup can be seen from Figure 3.16b.



**a) freeze/thaw chamber**

**b) NDT E-meter**

**Figure 3.16. Setup used for freeze/thaw resistance test.**

### 3.8.2 Surface and bulk resistivity

One cylinder specimen was randomly selected from each mixture to be tested for the surface (Figure 3.17a) and bulk resistivity (Figure 3.17b) using a Proceq Resipod testing device at 28 days based on AASHTO TP95 (Standard Method of Test for Surface Resistivity Indication of Concrete's Ability to Resist Chloride Ion Penetration). The Resipod works based on the Wenner probe principles and measures the electrical

resistivity of concrete. The specimen needs to be at fully saturated condition. Electric current is applied through the outer probes, while the inner probes measure the voltage.



**a) surface resistivity**

**b) bulk resistivity**

**Figure 3.17. Resistivity test setup.**

### 3.8.3 Free shrinkage

Three shrinkage bars of dimensions 3" by 3" by 11.25" were cast per mixture for free shrinkage testing according to ASTM C157 (Standard Test Method for Length Change of Hardened Hydraulic-Cement Mortar and Concrete). Specimens were cured until 28 days age, and then stored in environmental chamber with 73°F (22.8 °C) and 50% R.H. The initial reading was taken right after the specimens were moved from the curing room to the environmental chamber using the length comparator (see Figure 3.18). The average value from three specimens was recorded. The next readings were taken at 1, 3, 7, 14, and 28 days after the initial reading.



**Figure 3.18. Length comparator used for shrinkage measurement**

#### 3.8.4 Restrained shrinkage

One concrete ring was cast per mixture for restrained shrinkage testing in accordance with ASTM C1581 (Standard Test Method for Determining Age at Cracking and Induced Tensile Stress Characteristics of Mortar and Concrete under Restrained Shrinkage). One of the test specimens is shown in Figure 3.19a as an example. The specimens were stored in an environmental chamber with 73°F (22.8 °C) temperature and 50% R.H. for 28 days or until the stress release due to concrete cracking is noticeable. As shown in Figure 3.19b, the strain gauges were attached to the inner side of the steel ring using special adhesive and then were covered with wax coating. The readings were taken every one hour and monitored for sudden strain reduction. The age at which cracking occurred was reported to the nearest 0.25 day.



**a) Test specimen**

**b) Strain gauge attached to the steel ring**

**Figure 3.19. Restrained shrinkage test setup**

## CHAPTER 4. EXPERIMENTAL DESIGN AND RESULTS

### 4.1 Introduction

The objective of this chapter is to present the details of the testing plan development and results obtained from the experimental study. The scope of the work includes aggregate analysis and three phases on concrete study, which are aggregate blend investigation, performance of concrete with reduced cement content, and durability evaluation.

The first step was to analyze different aggregate matrices for East NE and West NE blends by using experimental and theoretical particle packing methods. Experimental packing degrees were obtained using the combined void content test and then compared to packing degrees obtained from the Modified Toufar Model.

Once various aggregate systems were evaluated, promising blends were selected for further investigation. A testing matrix was developed and consisted of three phases. Phase 1 included evaluating performances of concrete mixtures with promising aggregate blends at standard cement content. Blends that showed better performance were selected to proceed further to Phase 2, where cement content was reduced at 0.5 sack steps. Once the first two phases were completed, selected promising mixtures were tested for performance evaluation, which mainly focused on durability tests.

Finally, once all the results were collected and evaluated, corresponding conclusions were drawn, and some recommended changes to NDOT specifications of pavement concrete were proposed.

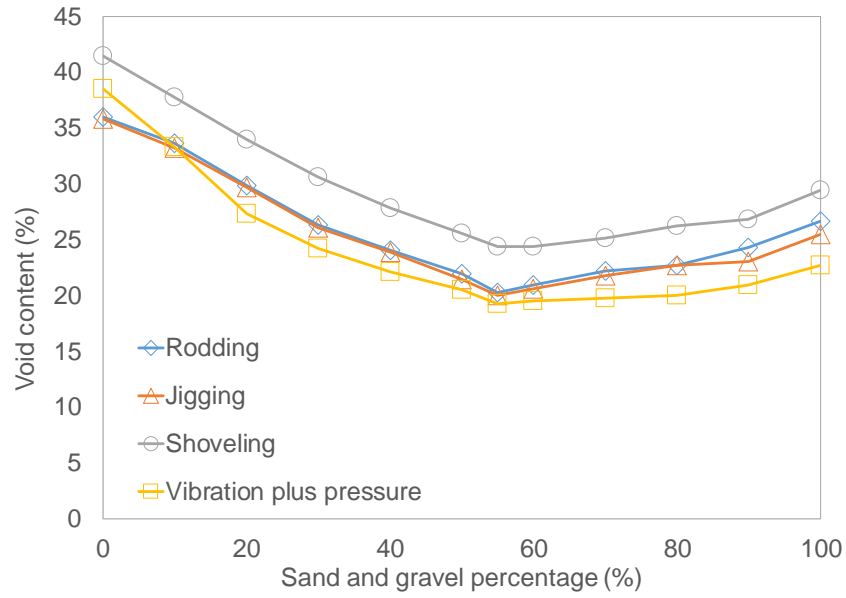


## 4.2 Aggregate system evaluation and selection

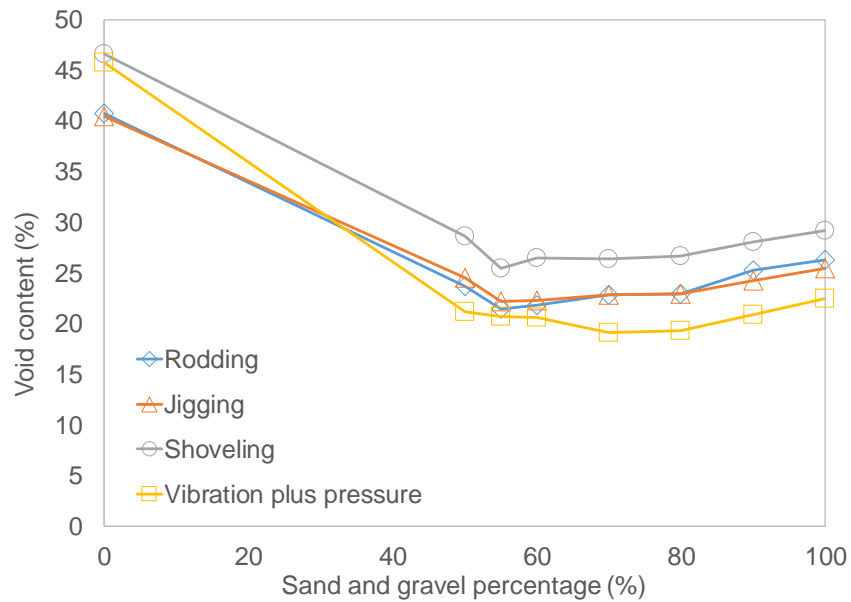
### 4.2.1 Experimental packing results

In order to develop a testing matrix, the aggregate system was first analyzed in terms of experimental particle packing. As shown in Figure 4.1, as expected and with the exception of the LS only case, the condition of vibration plus pressure resulted in a higher degree of compaction, followed by jiggling, rodding, and shoveling, respectively.

According to Figure 4.1a, the blend with the maximum packing is 55SG-45LS (identification represents a 55% SG and 45% LS blend) followed by promising blends as 60SG-40LS and 50SG-50LS. In terms of the West NE aggregate system, based on the experience from East NE aggregates system analysis, along with the results of blends  $SG\_W/A > 0.50$ , it was determined that the optimum blend would not be a blend with  $SG\_W/A < 0.50$ . To minimize the experimental effort, experimental tests for blends  $SG\_W/A < 0.50$  were not performed. From Figure 4.1b, it can be observed that the vibration plus pressure method resulted in 70SG<sub>W</sub>-30GR (identification represents a 70% SG<sub>W</sub> and 30% GR blend) as the optimum blend, while the other three methods showed that the blend with the lowest amount of voids is 55SG<sub>W</sub>-45GR.



**a) East NE blends void contents**



**b) East NE blends void contents**

**Figure 4.1. Results of the combined aggregate void content test**

#### 4.2.2 Theoretical packing results

Results from the theoretical packing degree were compared with the experimental results from the four different compaction methods. According to the individual void contents of SG, LS, SG\_W, and GR, together with the volume fractions of aggregates in different combinations, the theoretical packing degree can be calculated based on the modified Toufar Model as described earlier in Equation (2.4). As shown in Figures 4.2 and 4.3, there is a positive correlation between the experimental and theoretical packing degrees in the blends. From the East NE aggregate system analysis, it was determined that no clear correlation resulted from proportions of limestone exceeding 50% (such as SG/A<0.50), with the only apparent exception being via the vibration plus pressure method. Moreover, the maximum theoretical and experimental packing degree matched only when vibration plus pressure is used, which is 55SG-45LS. Regarding West NE aggregates system analysis, results showed that the optimum blend is whether 55SG\_W-45GR is based on the vibration plus pressure method or 70SG\_W-30GR is based on the other three methods. Besides the successful match with the theoretical packing, as mentioned earlier, it is believed that the vibration plus pressure method is the most representative method for pavement concrete applications procedure. Thus, the void contents from this procedure were used in throughout the remainder of the study.

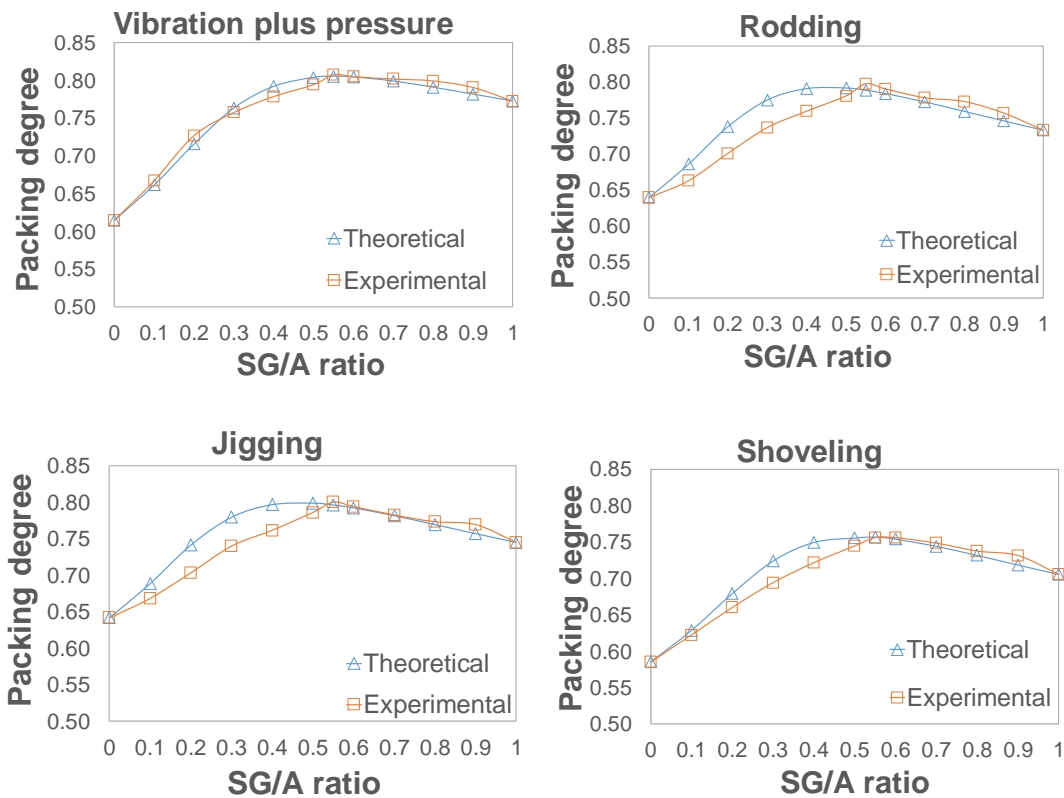


**Figure 4.2. Comparison between experimental and theoretical packing degrees of East NE blends**

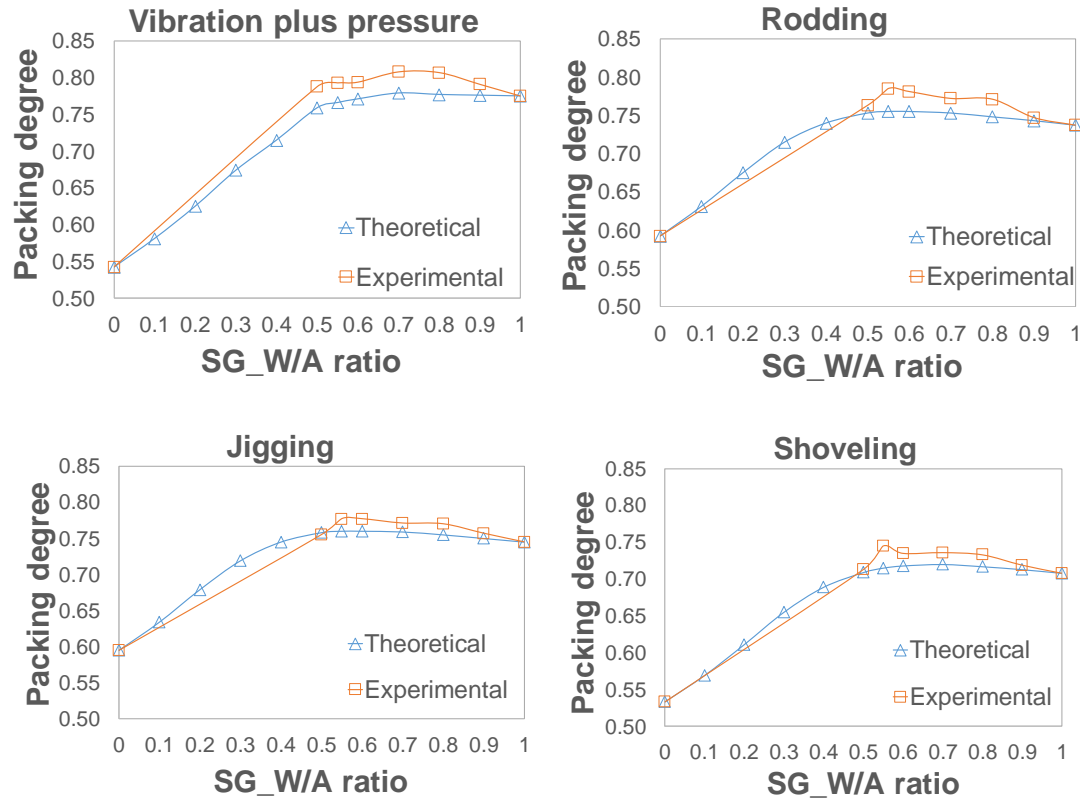


**Figure 4.3. Comparison between experimental and theoretical packing degrees of West NE blends**

### 4.3 Testing matrix development

After the particle packing analysis was completed, 70SG-30LS (reference), 60SG-40LS, 55SG-45LS, 50SG-50LS blends from East NE, and 70SG\_W-30GR, 55SG\_W-45GR blends from West NE were selected for concrete mixtures. These blends were also examined to determine if they satisfied the Tarantula Curve criteria (see Figure 4.4). It can be seen that the reference blend is out of the Tarantula limits with an excess of No. 8 and No. 16 particles. It is worth noting that one of the promising blends with West NE aggregates (70SG\_W-30GR) based on the combined aggregate void content test and Modified Toufar Model is out of Tarantula limits too, with an abundance of #8 and #16 size particles.

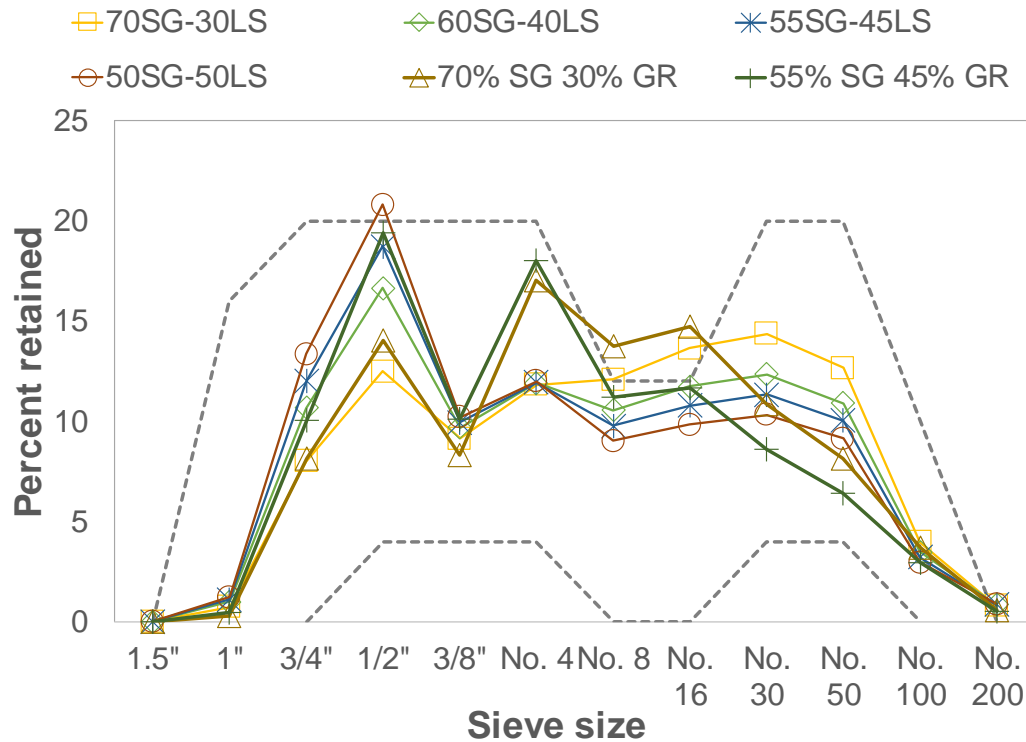


**Figure 4.4. Reference blend and blends chosen for further study plotted on Tarantula curve.**

In order to evaluate the impacts of aggregate gradation and cement content on pavement concrete performance, the testing matrix was divided into three Phases. Phase 1 was focused on obtaining the best blend performance while keeping the cement content at a standard 6.0 sacks (564 lb/yd<sup>3</sup>). The best blend was selected mainly based on the highest amount of excess paste shown in the box test performance and meeting the minimum mechanical property criteria. In Phase 1 mixes, the following blends were evaluated: 70SG-30LS (reference mix), 60SG-40LS, 55SG-45LS, and 50SG-50LS from East NE, and 70SG\_W-30GR, 55SG\_W-45GR from West NE. Once Phase 1 was completed, the most promising mixtures would be obtained. In Phase 2, promising blends along with the reference one were subjected to a stepwise reduction of cement content.

The cement factor was reduced by 0.5 sack (47 lb/yd<sup>3</sup>) steps, i.e., from 6.0 sacks (564 lb/yd<sup>3</sup>), to 5.5 sacks (517 lb/yd<sup>3</sup>), 5.0 sacks (470 lb/yd<sup>3</sup>) and 4.5 sacks (423 lb/yd<sup>3</sup>) and so on. After Phase 2, promising mixtures with reduced cement content were selected and, along with the reference mixture, were evaluated for performance. Performance evaluation included setting time, air content, modulus of elasticity, resistance to freeze/thaw cycles, drying shrinkage, and restrained shrinkage tests.

#### 4.4 Excess Paste/Aggregates Calculation

To achieve appropriate workability, simply filling voids among aggregate particles with cement paste is not sufficient, and an excess amount of paste is needed to cover aggregates. The amount of excess paste depends on the paste quality and surface area of aggregate particles (Kennedy, 1940). Due to the varied specific gravity of aggregates, two different aggregates with the same mass may differ in volume occupied in a mix. Therefore, to be able to compare mixes more objectively, it is more reasonable to consider the excess paste/aggregates ratio.

Once the bulk density and void content of a particular blend of aggregate is known, the excess paste in a mix can be calculated. The first step was to calculate the aggregate's bulk volume ( $V_{B\_agg}\%$ ) as presented in a mix by dividing the total mass of aggregates in a specific concrete mix design ( $M_t$ , in lb/yd<sup>3</sup>) with the bulk density of a blend ( $D_b$ , in lb/ft<sup>3</sup>) and 27 (ft<sup>3</sup>/yd<sup>3</sup>).

$$V_{B\_agg}\% = \frac{M_t / D_b}{27} \quad (4.1)$$

Then, the void content in a mix ( $VO_{mix}\%$ ) was obtained by multiplying the volume of aggregate in concrete by the void content in the aggregate blend ( $VO_{blend}\%$ ).

$$VO_{mix}\% = V_{B\_agg}\% \times VO_{blend}\% \quad (4.2)$$

As the air content in the cement paste is often unknown, which makes it difficult to calculate the paste volume directly, the total paste volume ( $P_t\%$ ) was calculated by subtracting the coarse and fine aggregate volumes from the total volume of concrete (100%). The aggregate volumes were calculated by dividing the mass of aggregate ( $M_1$  or  $M_2$ , in lb/yd<sup>3</sup>), by the specific gravity ( $G_{sb1}$  or  $G_{sb2}$ ) times the specific gravity of water (at 62.4 lb/ft<sup>3</sup>) and then divided by 27 (ft<sup>3</sup>/yd<sup>3</sup>).

$$P_t\% = 100\% - \frac{M_1/(G_{sb1} \times 62.4pcf)}{27} - \frac{M_2/(G_{sb2} \times 62.4pcf)}{27} \quad (4.3)$$

The last step was to obtain the excess paste volume ( $P_e\%$ ) by subtracting  $VO_{mix}\%$  from the total paste volume in the mix ( $P_t\%$ ).

$$P_e\% = P_t\% - VO_{mix}\% \quad (4.4)$$

Finally, the excess paste-to-aggregate volume ratio ( $P_e\%/V_{B\_agg}\%$ ) can be calculated by dividing  $P_e\%$  by  $V_{B\_agg}\%$ .

## 4.5 Phase 1 Results

### 4.5.1 Mix proportions

Table 4.1 shows the mix proportions for mixtures included in Phase 1. The mix identification is based on three parameters, i.e., cement content in sacks (C) and the fractions of SG and LS. As an example, C6SG70LS30 stands for a mixture with a cement content of 6.0 sacks, SG fraction of 70, and LS fraction of 30 (Figure 4.5). Water-to-cement ratio (w/c) was fixed at 0.43 for East NE mixes. For West NE mixes it was decided to use a lower w/c at 0.41. The calculated total paste volume ( $P_t\%$ ), excess paste



volume ( $P_c\%$ ), and excess paste-to-aggregate volume ratio ( $P_e\%/V_{B\_agg}\%$ ) are also shown in Table 4.1.

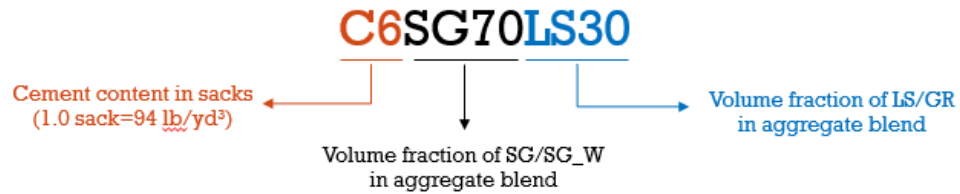


**Figure 4.5. Mix identification**

**Table 4.1. Mix proportions for mixes of Phase 1**

	Mix ID	w/c	CF	LS/GR	SG/SG_W	Water	AEA	WR	P <sub>t</sub> %	P <sub>c</sub> %	P <sub>e</sub> %/V <sub>B_agg</sub> %
East	C6SG70LS30	0.43	564	912	2060	243	0.125	0.0	31.88	14.91	0.17388
	C6SG60LS40	0.43	564	1216	1766	243	0.125	0.0	31.89	15.24	0.17840
	C6SG55LS45	0.43	564	1368	1619	243	0.125	0.0	31.88	15.52	0.18231
	C6SG50LS50	0.43	564	1520	1472	243	0.125	0.0	31.88	14.11	0.16300
West	C6SG_W70GR30	0.41	564	897	2027	231	3.00	0.0	32.33	16.28	0.19425
	C6SG_W55GR45	0.41	564	1345	1592	231	4.00	2.5	32.49	14.83	0.17388

Note: all ingredients are in lb/yd<sup>3</sup>, except for the chemical admixtures (WR and ARA), which are in fl oz/cwt (1 lb/yd<sup>3</sup>= 0.5935 kg/m<sup>3</sup>, 1 fl oz/cwt= 0.6519 mL/kg)

#### 4.5.2 Fresh concrete properties

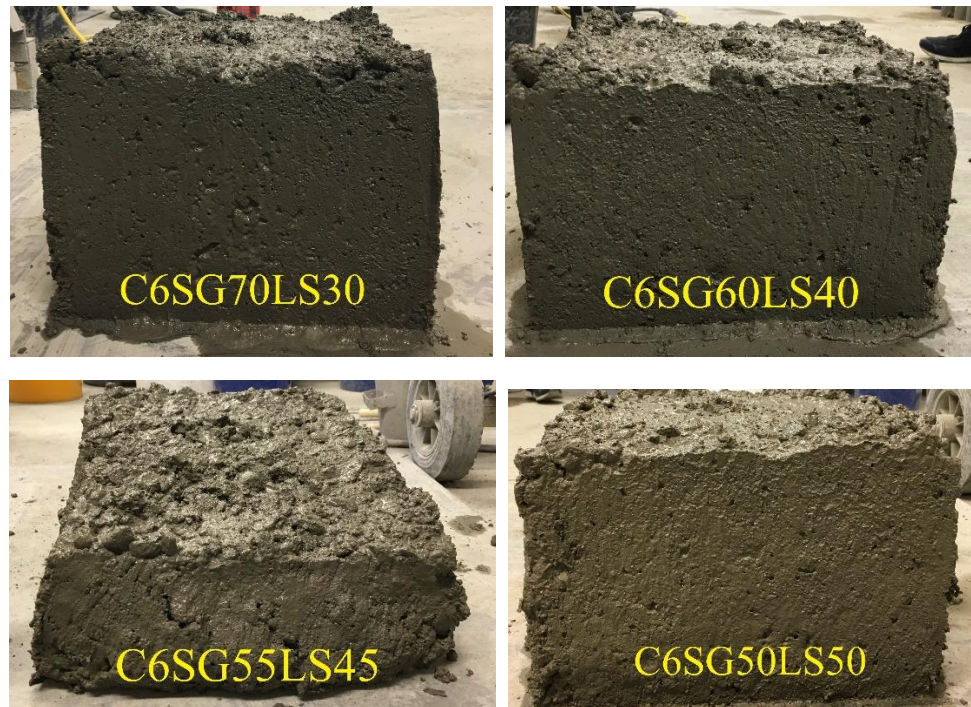
Fresh concrete properties, with a particular focus on the results of the Box Test, were used as the main criteria to select the most promising blend. Table 4.2 summarizes fresh concrete properties of Phase 1 mixes. In addition, Box Test images for all mixes are shown in Figure 4.6. Results revealed that all six mixes have low surface void content, which indicated sufficient paste content to cover the aggregates. Also of note: although results shown below presented a lower box ranking for the C6SG55LS45 mix, it was still considered to be a more promising blend. Even though the mix was considered failed per

the Box Test, it was apparently largely due to the high amount of excess paste. This result also indicated that less paste is necessary for this mix.

**Table 4.2. Fresh concrete properties of Phase 1 mixes**

Mix ID	East				West	
	C6SG70 LS30	C6SG60 LS40	C6SG55 LS45	C6SG50 LS50	C6SG_W 70GR30	C6SG_W 55GR45
# of adjustments	0	0	0	0	0	1
Slump (in)	1.5	2.5	5	3.5	4	4
Box test ranking	1	1	failed	2	1	1
Surface voids (%)	3.8	3.6	NA	3.7	2.7	2.5
Revised box test ranking	E1-S2	E1-S2	E4b-S4	E3-S2	E2-S1	E3-S1
Vindex	0.346	0.447	0.365	0.562	0.563	0.472

Note: 1 in= 25.4 mm



a) Box test images for East NE mixes



b) Box test images for West NE mixes

Figure 4.6. Box test images from Phase I mixes

## 4.6 Phase 2 Results

### 4.6.1 Mix proportions

In terms of East NE mixes, based on results obtained in Phase 1, the blend selected for further investigation (along with the reference blend) is 55SG-45LS.

Regarding the West NE mixes, as it was not that clear which blend is the optimum, it was decided to proceed with both blends. Mixtures with a stepwise reduction of 0.5 sacks of

cement from 6.0 sacks to 4.5 sacks were developed. Mix proportions for both East NE and West NE mixes are presented in Table 4.3. For East NE mixes, w/c was increased to 0.45 in this phase to accommodate the anticipated reduction of workability due to the reduction of cement content. For West NE mixes, it was decided to keep w/c the same as in Phase 1.

**Table 4.3. Mix proportions for mixes of Phase 2**

	Mix ID	w/c	CF	LS/GR	SG/SG_W	Water	AEA	WR	P <sub>t</sub> %	P <sub>e</sub> %	P <sub>e</sub> %/V <sub>B,agg</sub> %
East	C6SG70LS30	0.43	564	912	2060	243	0.125	0.0	31.88	14.91	0.17388
	C6SG55LS45	0.43	564	1368	1619	243	0.125	0.0	31.88	15.52	0.18231
	CS5.5SG70LS30	0.45	517	942	2128	233	0.125	4	30.21	12.83	0.14609
	CS5.5SG55LS45	0.45	517	1413	1672	233	0.125	0	30.21	13.46	0.15438
	CS5SG70LS30	0.45	470	972	2196	212	0.125	20	28.02	10.09	0.11129
	CS5SG55LS45	0.45	470	1458	1725	212	0.125	4	28.02	10.74	0.11937
	CS4.5SG55LS45	0.45	423	1504	1779	190	0.125	24	25.75	7.93	0.08542
West	C6SG_W70GR30	0.41	564	897	2027	231	3.00	0.0	32.33	16.28	0.19425
	C6SG_W55GR45	0.41	564	1345	1592	231	4.00	2.5	32.49	14.83	0.17388
	C5.5SG_W70GR30	0.41	517	925	2089	212	4.000	5	31.37	14.82	0.17162
	C5.5SG_W55GR45	0.41	517	1388	1642	212	4.000	8	31.36	13.14	0.14935
	C5SG_W70GR30	0.41	470	952	2154	193	1.500	8	28.75	11.70	0.13142
	C5SG_W55GR45	0.41	470	1430	1691	193	1.500	8	28.90	10.14	0.11182
	C4.5SG_W70GR30	0.41	423	981	2217	173	0.500	12	26.79	9.23	0.10074

Note: all ingredients are in lb/yd<sup>3</sup>, except for the chemical admixtures (WR and ARA), which are in fl oz/cwt (1 lb/yd<sup>3</sup>= 0.5935 kg/m<sup>3</sup>, 1 fl oz/cwt= 0.6519 mL/kg)

#### 4.6.2 Fresh concrete properties

Table 4.4 presents fresh concrete test results for East NE mixes and Box Test images are shown in Figure 4.7. It can be noted that for the reference blend with 0.5 sacks of reduced cement (C5.5SG70LS30), a WR adjustment of 4fl oz/cwt was needed to pass the Box Test. In comparison, mixes with the optimum blend (C5.5SG55LS45)

resulted in a good performance without any WR addition, solidifying that 55SG-45LS is the optimum gradation. When cement was reduced by 1.0 sack for the reference blend (C5SG70LS30), even four adjustments for a total WR dosage of 20 fl oz/cwt was not sufficient to pass the Box Test, and the final box test ranking was E3-S3. For the C5SG55LS45 mix, a minimum WR dosage of 4 fl oz/cwt was necessary to obtain an acceptable mixture and resulted in an E2-S2 ranking. Results of East NE mixes suggest that by introducing a higher amount of LS that is more angular compared to SG, the improved gradation and decreased surface area of aggregates helped to reduce the needed cement content. Results showed that it is not feasible to obtain an acceptable mixture for the optimized blend with 1.5 sacks of cement (C4.5SG55LS45) reduced, even with the WR. It is then reasonable to assume that 5.0 sacks of cement is the minimum cement content with the materials used in this series.

Fresh concrete properties and images from the Box Test for West NE mixes are demonstrated in Table 4.5 and Figure 4.8, respectively. In general, both blends worked appropriately with a 0.5 and 1.0 sack of cement reduction. However, it can be seen that 70SG\_W-30GR blend resulted in slightly better performance, indicating that it is the optimum blend for the aggregates in this series. It could be due to the fact that GR is more angular compared to LS, thus negatively affecting particle packing. The observation is consistent with results from the theoretical and experimental particle packing as shown in Figure 4.1 and 4.3. It is important to note that while the Tarantula Curve showed the 55SG\_W-45GR blend to be the optimum, results from the Modified Toufar Model and experimental test with vibration plus pressure method to predict the packing were deemed

more accurate. The reasoning likely being that the Tarantula Curve takes into account gradation while ignoring aggregate shape.

**Table 4.4. Fresh concrete properties of Phase 2 East NE mixes**

Mix ID	C6SG70 LS30	C6SG55 LS45	C5.5SG70 LS30	C5.5SG55 LS45	C5SG70 LS30	C5SG55 LS45	C4.5SG55 LS45
Number of adjustments	0	0	1	0	4	1	3
Slump (in)	1.5	5	2.5	4	1	2	0
Box test ranking	1	failed	1	1	3	3	failed
Surface voids (%)	3.8	NA	3.1	2.3	8.9	3.2	NA
Revised box test ranking	E1-S2	E4b-S4	E1-S2	E2-S1	E3-S3	E2-S2	E4a-S4
$V_{index}$	0.346	0.365	0.354	0.532	0.353	0.424	0.434

Note: 1 in= 25.4 mm

**Table 4.5. Fresh concrete properties of Phase 2 West NE mixes**

Mix ID	C6SG_ W70GR 30	C6SG_ W55GR 45	C5.5SG _W70G R30	C5.5SG _W55G R45	C5SG_ W70GR 30	C5SG_ W55GR 45	C4.5SG _W70G R30
Number of adjustments	0	1	1	2	1	1	2
Slump (in)	4	4	2.25	3.5	3	4.25	0.75
Box test ranking	1	1	1	2	1	2	4
Surface voids (%)	2.7	2.5	2.7	3.7	2.5	3.4	10.5
Revised box test ranking	E2-S1	E3-S1	E2-S1	E2-S2	E2-S1	E2-S2	E4a-S3
$V_{index}$	0.563	0.472	0.362	0.427	0.360	0.429	0.259

Note: 1 in= 25.4 mm

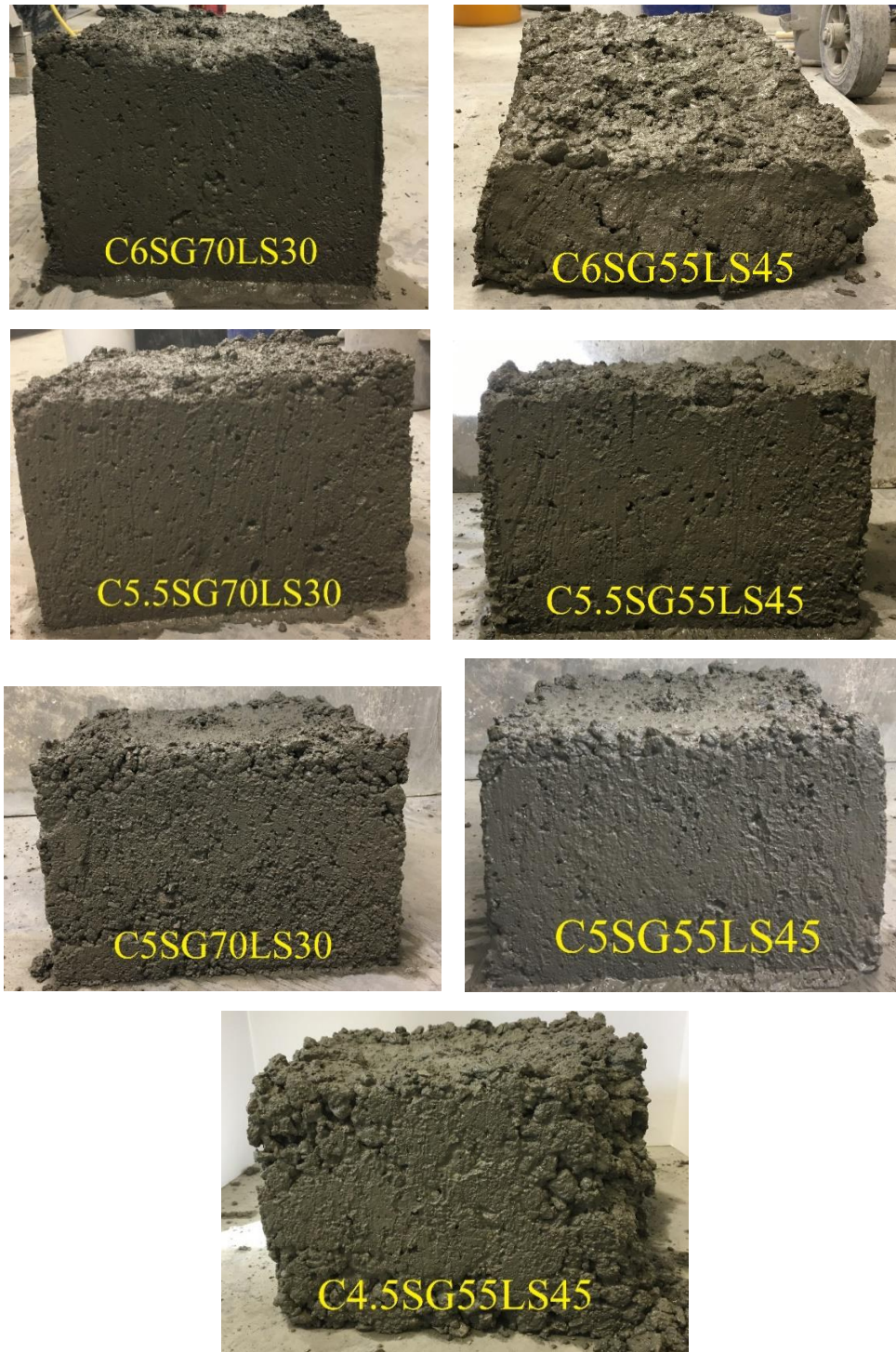


**Figure 4.7. Box test images for East NE mixes**

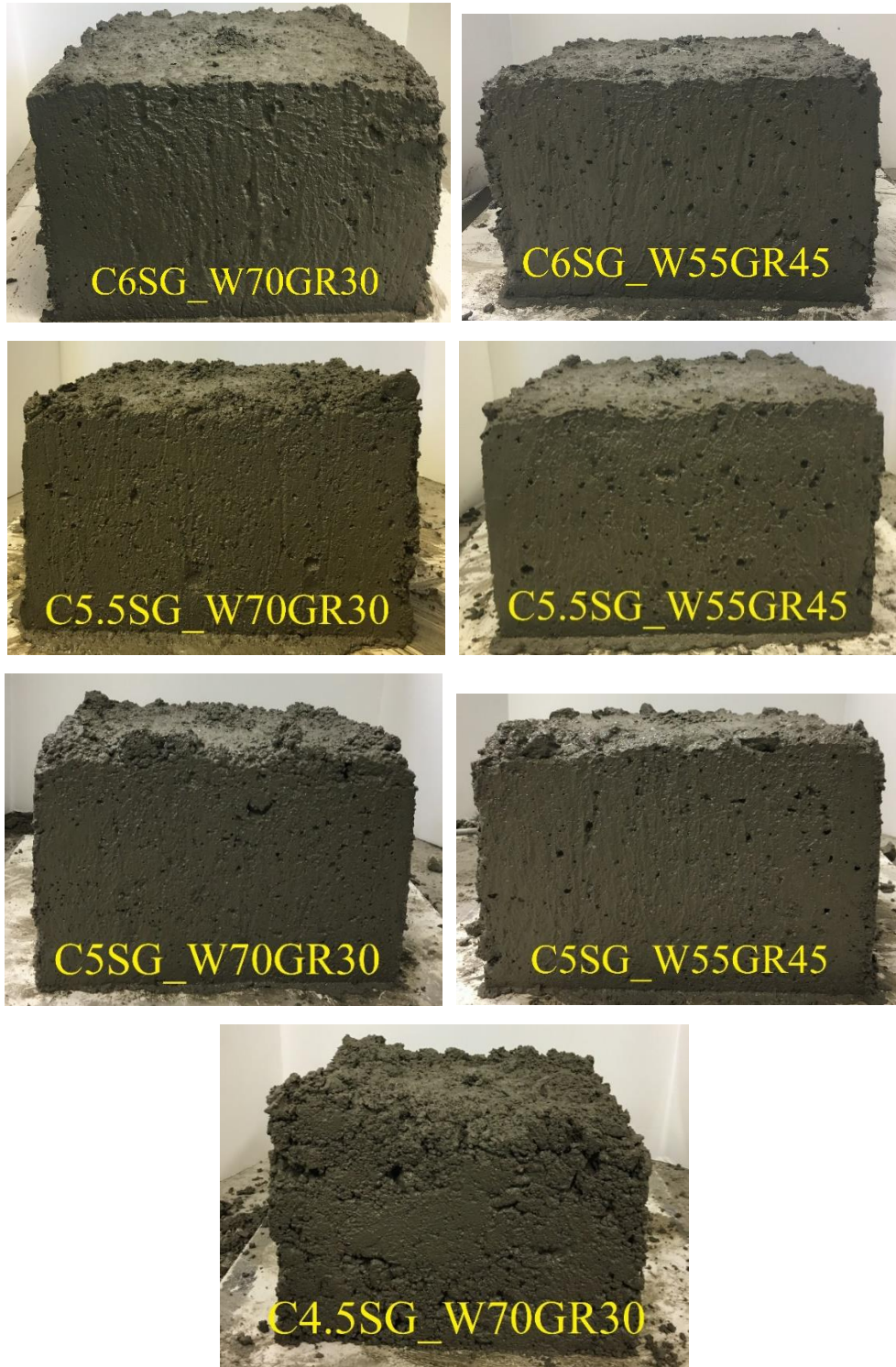
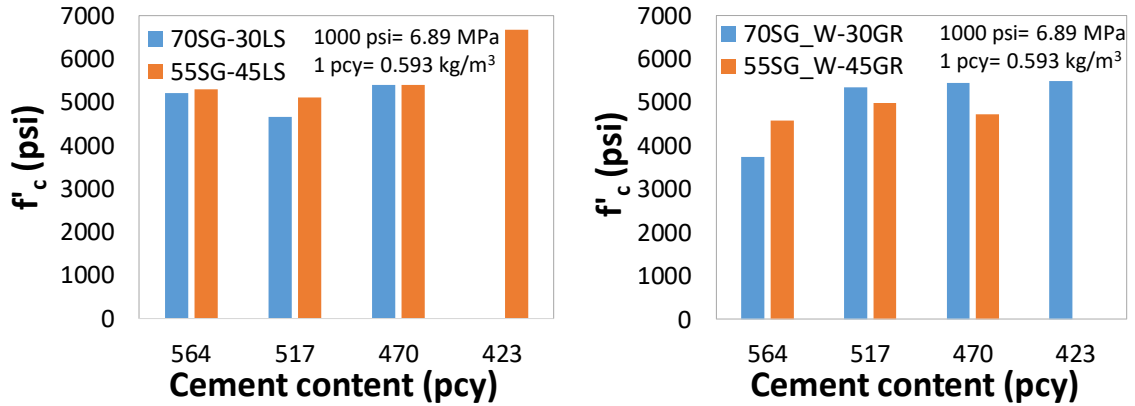


Figure 4.8. Box test images for West NE mixes

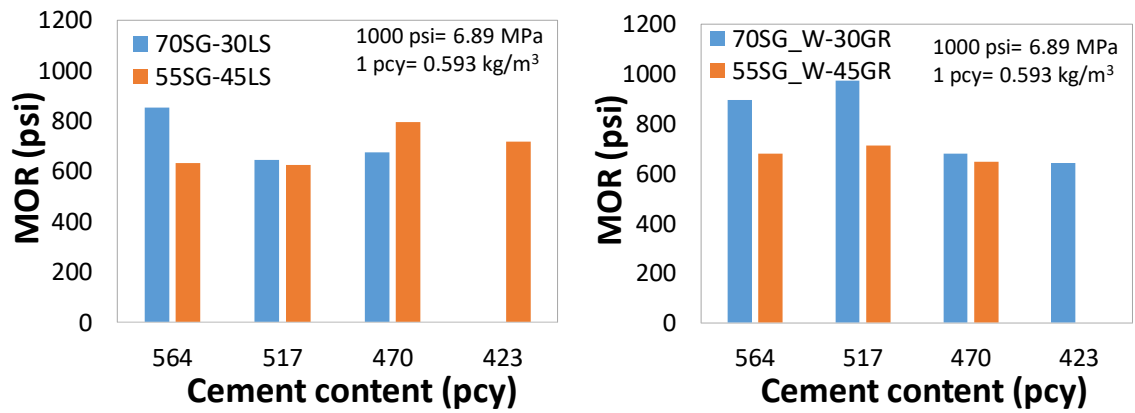


#### 4.7 Hardened concrete properties of Phases 1 and 2

In terms of hardened concrete properties, the effect of cement reduction on properties including compressive strength, modulus of rupture, and surface and bulk resistivity were evaluated. Note that even with the reduction of cement content, there is no significant change in strength (Figure 4.9a). These results are consistent with Yurdakul (2010) and Wassermann et al. (2009). There is also no significant effect of cement content on the modulus of rupture (Figure 4.9b). West NE mixes resulted in slightly higher flexural strength. This may be due to the more angular aggregate used. The developed mixes were all deemed acceptable based on the minimum compressive strength and modulus of rupture at 28 days specified for pavements in Nebraska, which are 3,500 psi and 600 psi, respectively. Surface and bulk resistivity are also not compromised by the reduction of cement content (Figure 4.10). However, values seem to be relatively low, which is believed to be due to high pozzolan content in mixes.

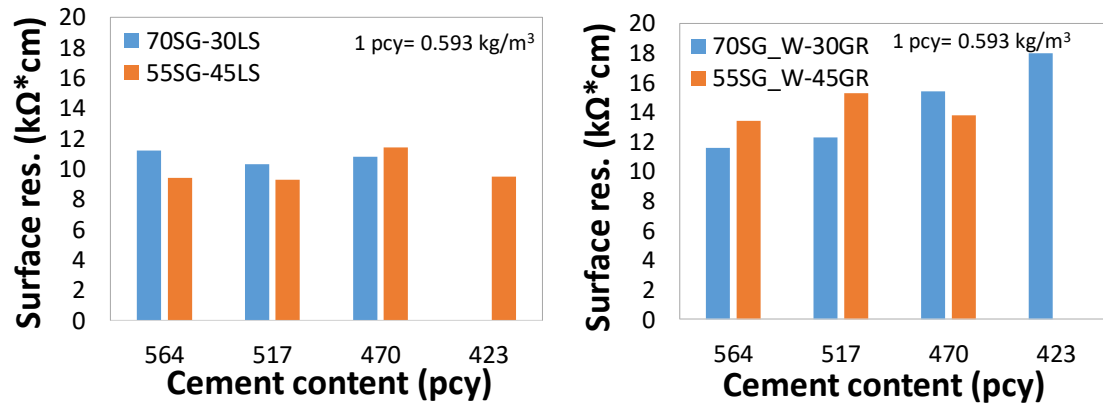


a) Effect of cement content on compressive strength ( $f'_c$ )

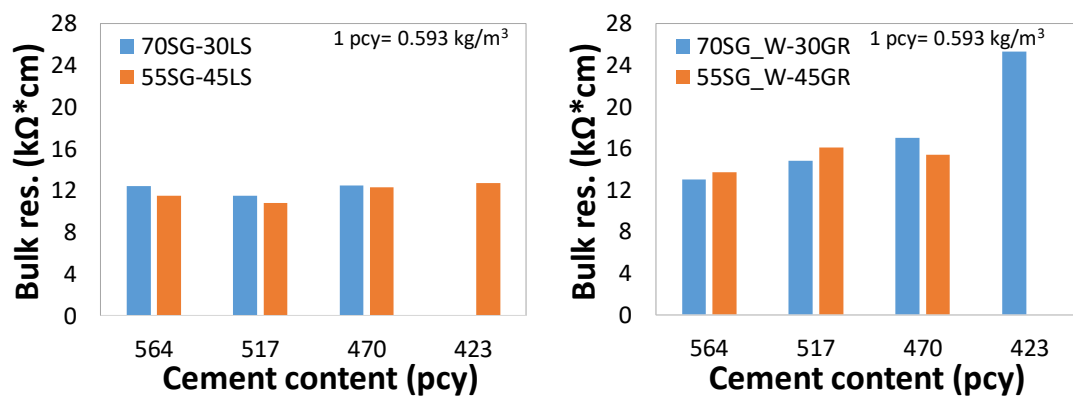


b) Effect of cement content on modulus of rupture (MOR)

Figure 4.9. Effect of cement content on mechanical properties



a) Effect of cement content on surface resistivity



b) Effect of cement content on bulk resistivity

Figure 4.10. Effect of cement content on permeability

## 4.8 Performance evaluation

### 4.8.1 Mix proportions

For performance evaluation, in addition to the reference mixture (C6SG70LS30), two East NE mixes (C5.5SG55LS45 and C5SG55LS45) were selected. Proportions of the aforementioned mixes are presented in Table 4.6.

**Table 4.6. Mix proportions for performance evaluation mixes**

Mix ID	w/c	CF	LS	SG	Water	AEA	WR
C6SG70LS30	0.41	564	904	2042	231	2.00	0.0
C5.5SG55LS45	0.41	517	1398	1654	212	2.50	0.0
C5SG55LS45	0.41	470	1438	1702	193	2.00	6.0

Note: all ingredients are in lb/yd<sup>3</sup>, except for the chemical admixtures (WR and AEA), which are in fl oz/cwt (1 lb/yd<sup>3</sup>= 0.5935 kg/m<sup>3</sup>, 1 fl oz/cwt= 0.6519 mL/kg)

#### 4.8.2 Fresh concrete and mechanical properties

Fresh concrete properties of performance evaluation mixes are tabulated in Table 4.7. NDOT Standard Specifications for Highway Construction (2017) require 6.5-9.0% of air in pavement mixes. It can be seen that air content obtained in all three mixes is within an acceptable range. In terms of setting time, it can be noticed that both initial and final sets of C5.5SG55LS45 happened slightly earlier when compared to the reference mix, which can be explained by a lower amount of cement paste volume. Mix C5SG55LS45 showed a dramatic increase in initial and final set time with even lower cement content, which is believed to be caused by the presence of WR, which can delay hydration and extend initial and final sets.

**Table 4.7. Fresh concrete properties of performance evaluation mixes**

Mix ID	C6SG70LS30	C5.5SG55LS45	C5SG55LS45
Slump (in)	3.0	3.5	4.5
Air content (%)	7.0	7.2	8.0
Initial set (min)	275	255	395
Final set (min)	395	380	520

Note: 1 in= 25.4 mm

In terms of mechanical properties, a modulus of elasticity test was performed. Results can be found in Figure 4.11. C5.5SG55LS45 resulted in a slightly higher elastic modulus, which may be due to a lower paste content and higher aggregates volume. However, C5SG55LS45, which had lower paste content and higher aggregate volume compared to C5.5SG55LS45, did not result in a higher elastic modulus. One of the possible reasons is the higher air content, which is believed to slightly lower modulus of elasticity. In general, all three mixes have very close results. It can be concluded that the reduction of cement content does not significantly influence the modulus of elasticity.

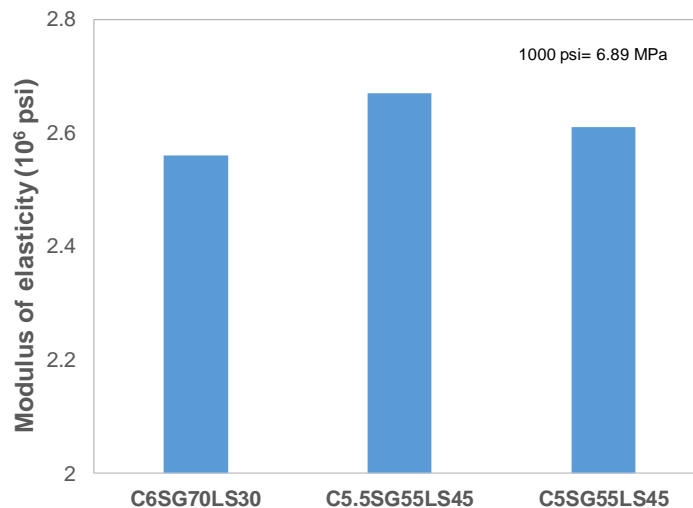
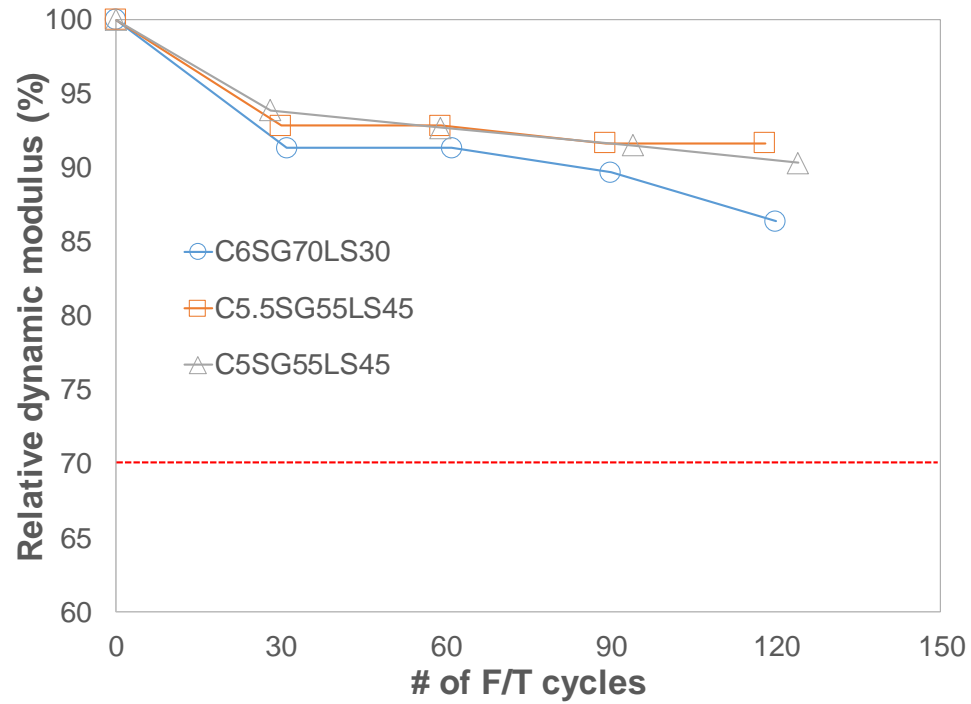


**Figure 4.11. Modulus of elasticity of reference and promising mixes**

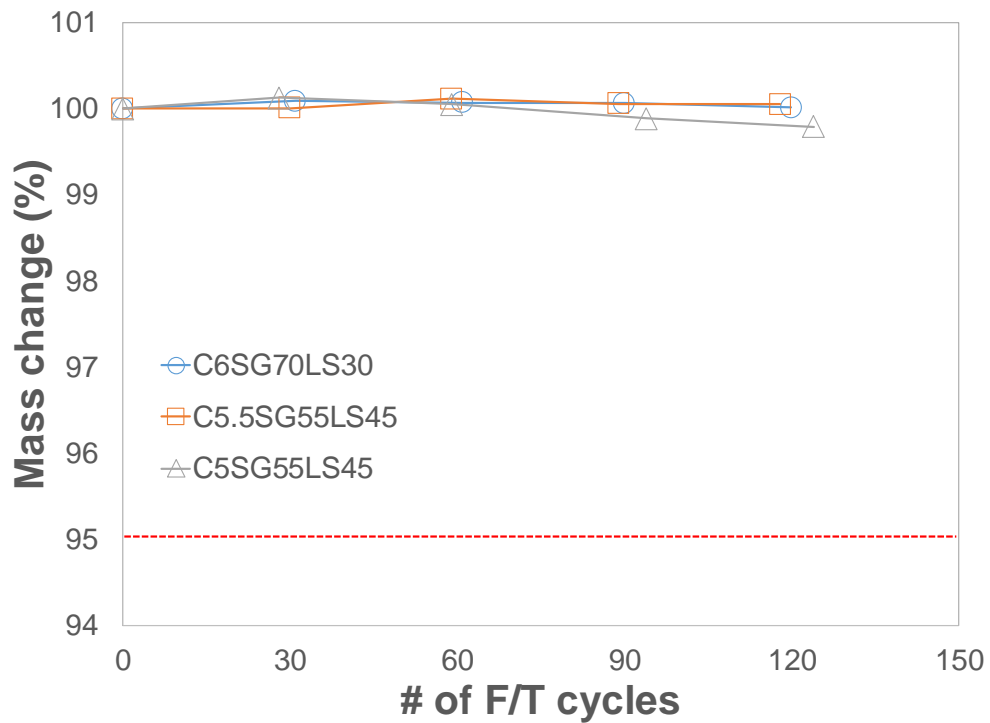
#### 4.8.3 Durability properties

Even though freeze/thaw resistance testing is still in progress, intermediate results are presented and discussed. Figure 4.12 demonstrates the relative dynamic modulus and mass change up to 120 cycles. From Figure 4.12a, it can be seen that mixtures with optimum gradation are demonstrating very similar performance despite the difference in cement content and air content. It can be stated that a 0.5 sack difference in cement content and 0.8% difference in air content does not significantly influence freeze/thaw

resistance. C5.5SG55LS45 and C6SG70LS30 have almost identical air content, and yet the optimum blend mixture is performing better. It is believed that mixtures with a higher amount of coarse aggregates have higher freeze/thaw resistance. NDOT specifies a minimum relative dynamic modulus of 70% at 300 cycles. Figure 4.12b illustrates mass change over freeze/thaw cycles. While there is no significant change in mass loss between the three mixes, it seems that 120 cycles is too early to draw any conclusions. NDOT specification requires no more than 5% of mass change at 300 cycles.



a) Relative dynamic modulus change



b) Mass change

Figure 4.12. Freeze/thaw resistance results up to 120 cycles

Figure 4.13 demonstrates results from the free shrinkage test. As expected, the reference mixture (C6SG70LS30) resulted in a higher shrinkage rate due to a higher cement paste volume. The difference at 28 days is about 50 and 90 microstrains compared to C5.5SG55LS45 and C5SG55LS45, respectively.

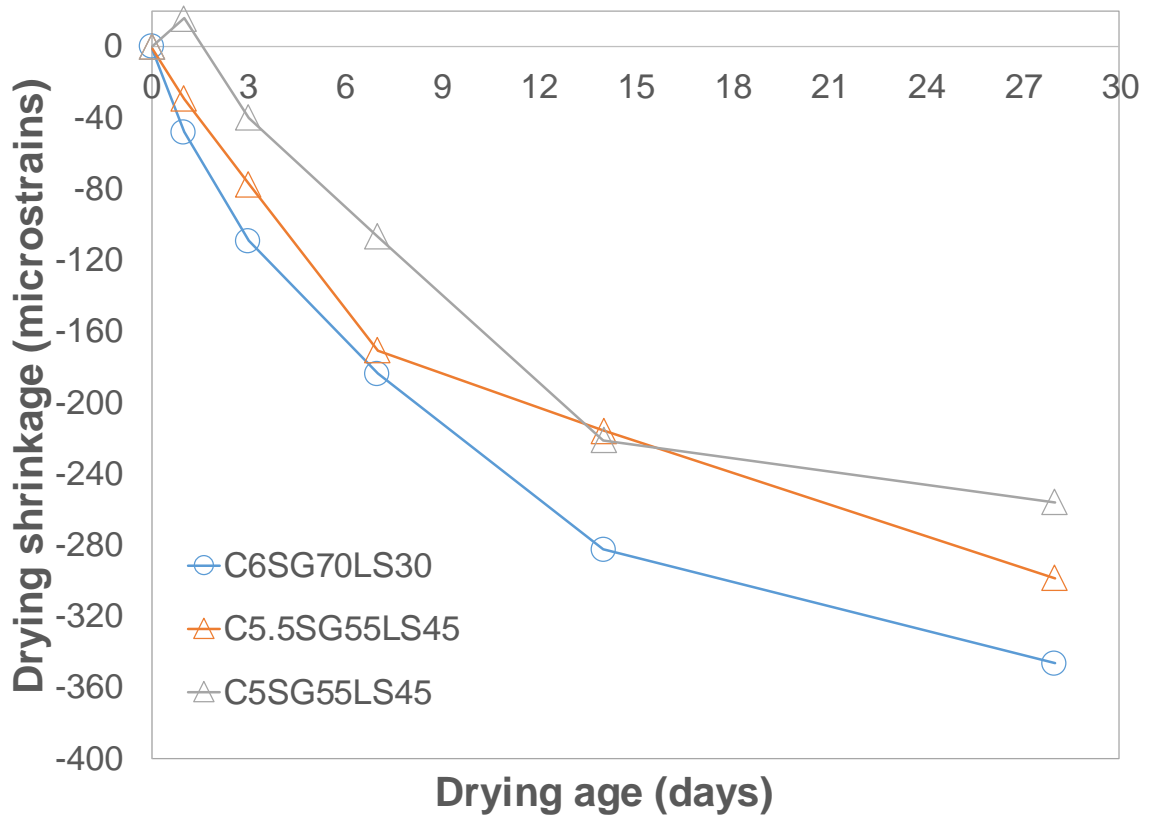


**Figure 4.13. Free shrinkage results up to 14 days**

Figure 4.14 shows the results of the restrained shrinkage test. As expected, with reduction of cement content, the age at cracking under restrained shrinkage increases. For C6SG70LS30, C5.5SG55LS45, and C5SG55LS45 the age at cracking was 11.5, 13.0, and 15 days, respectively.



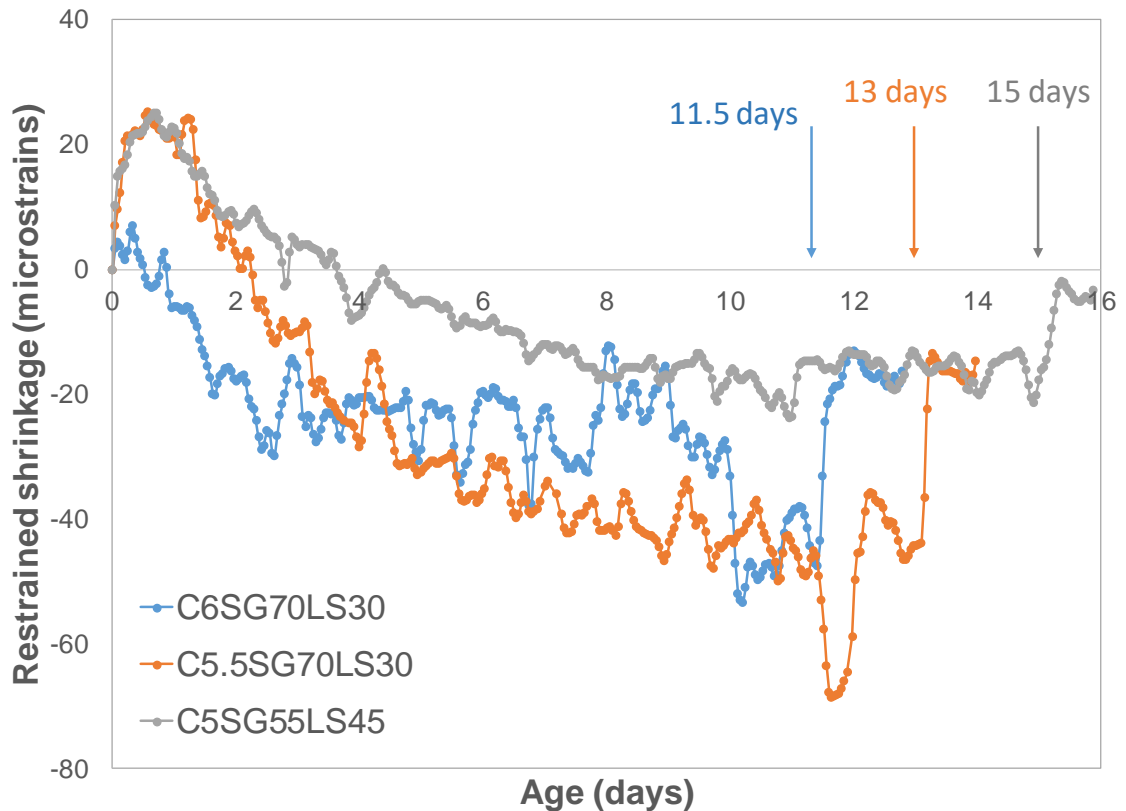


**Figure 4.14. Restrained shrinkage results**

#### 4.9 Proposed changes in NDOT specifications

Table 4.8 represents the main requirements for slip formed pavement concrete specified by NDOT (NDOT Standard Specifications for Highway Construction, 2017). From the results obtained in this study, it can be concluded that the requirement of the minimum amount of total cementitious materials can be reduced from 564 lb/yd<sup>3</sup> to 470 lb/yd<sup>3</sup> with the optimum gradation. If the minimum requirement for cementitious materials decreases, the maximum amount of total aggregate will increase. In this study, when the proposed minimum cementitious material amount was used, the total aggregate amount increased up to 3183 lb/yd<sup>3</sup>. Therefore, it seems reasonable to change the maximum requirement of the total aggregate amount from 3150 lb/yd<sup>3</sup> to 3200 lb/yd<sup>3</sup>.

**Table 4.8. NDOT specifications for pavement concrete mix (2017)**

Class of Concrete	Base Cement Type	W/C Ratio Max.	Total Cementitious Materials Min. (lb/yd <sup>3</sup> )	Total Aggregate		Coarse Aggregate (%)
				Min. (lb/yd <sup>3</sup> )	Max. (lb/yd <sup>3</sup> )	
47B	IP	0.45	564	2850	3150	-

#### 4.10 Summary

According to the aggregate systems evaluation through both experimental and theoretical packing analysis, it was justified that the reference blend, which is currently being used, does not provide the optimum gradation. Besides this, it was found that there is a high correlation between experimental and theoretical particle packing degrees when the vibration plus pressure method is used. It is believed that the Modified Toufar Model can be used to accurately predict the packing degree.

Based on the concrete mixtures performed, it was justified that aggregate gradation plays a significant role in fresh concrete performance. It was found that when optimum gradation is used, cement content can be reduced by up to 1.0 sacks. Mechanical properties were not compromised by cement content reduction and still met NDOT requirements. Durability tests showed that concrete mixtures with optimum blend have higher resistance to freeze/thaw cycles. It was also determined that reducing cement content leads to less shrinkage, which was demonstrated by both free and restrained shrinkage tests.

In summary, it can be concluded that cement content can be reduced when the optimum blend is used. In addition, better durability properties were achieved. According

to the results obtained, changes of the required cement and total aggregate contents to NDOT specifications were proposed.

## CHAPTER 5. MIX DESIGN IMPROVEMENT PROCEDURE

### 5.1 Introduction

This chapter includes a mixture design improvement procedure developed based on the results obtained in the previous chapter. Excess paste-to-aggregate ratio ( $P_e\%/V_{B\_agg}\%$ ) is used as the main control parameter to design a pavement concrete. The feasibility of using the Box Test and VKelly Test to justify pavement concrete workability is also analyzed, and corresponding conclusions are drawn. Finally, a simple four-step design improvement procedure is proposed.

### 5.2 Design philosophy

The design philosophy consists of a systematic selection of an aggregate system and designing concrete with the minimum possible cement content yet having mechanical and durability properties unaffected or improved. The main contribution of the developed improvement in mix design procedure is to use a theoretical particle packing model that accounts for aggregate shape and texture and then using  $P_e\%/V_{B\_agg}\%$  ratio as the main parameter to drive the mix design. In addition to this, it is important to evaluate pavement concrete workability with specific tests such as the Box and/or VKelly Tests.

Figure 1 presented the relationship among  $P_e\%/V_{agg}$ ,  $V_{index}$  from the VKelly Test, and surface voids from the Box Test. As shown in Figure 5.1a, there is no strong correlation between  $P_e\%/V_{agg}$  and  $V_{index}$ , which demonstrates that it is inappropriate to use the VKelly Test to guide mix design. Moreover, no clear trend can be observed in the graphical relationship between  $V_{index}$  from the VKelly Test and surface voids from the Box Test as shown in Figure 5.1b. It is believed that the VKelly Test is not a helpful test

for pavement concrete with the low coarse aggregate amount. The potential reason for this is insufficient coarse aggregate particles to support the Kelly ball.

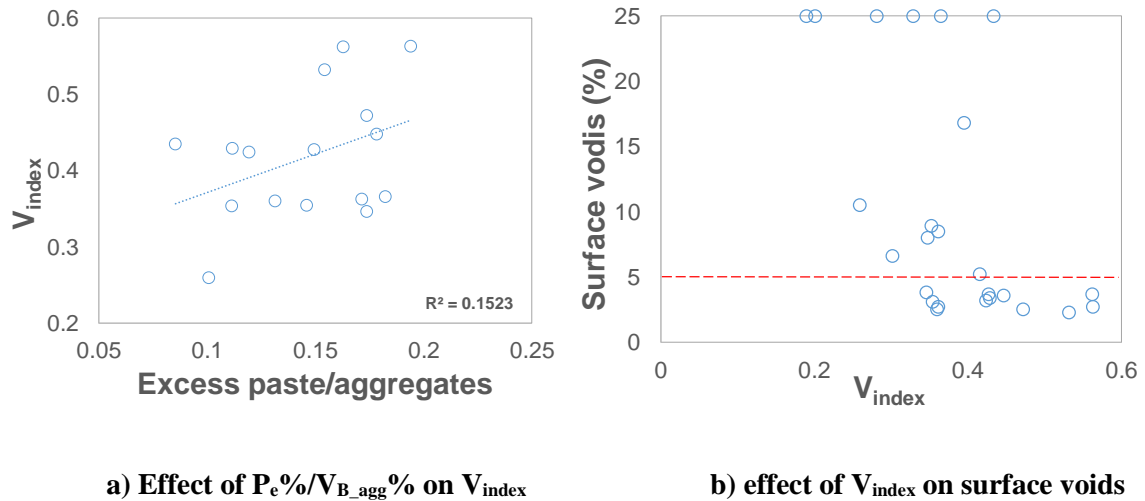
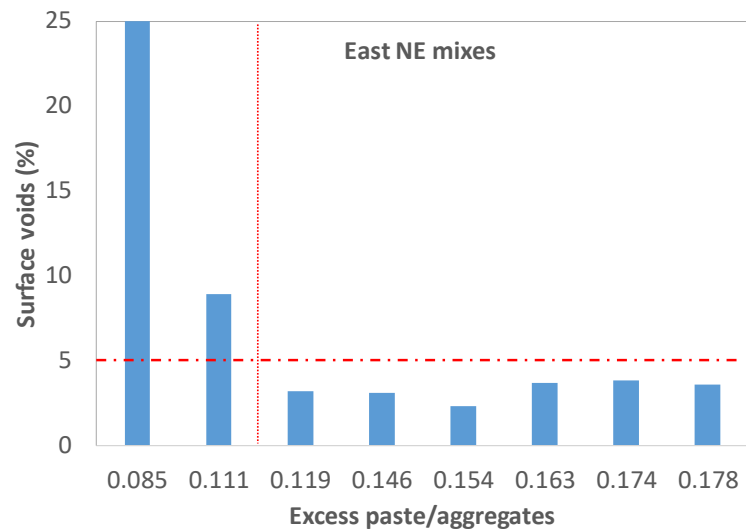


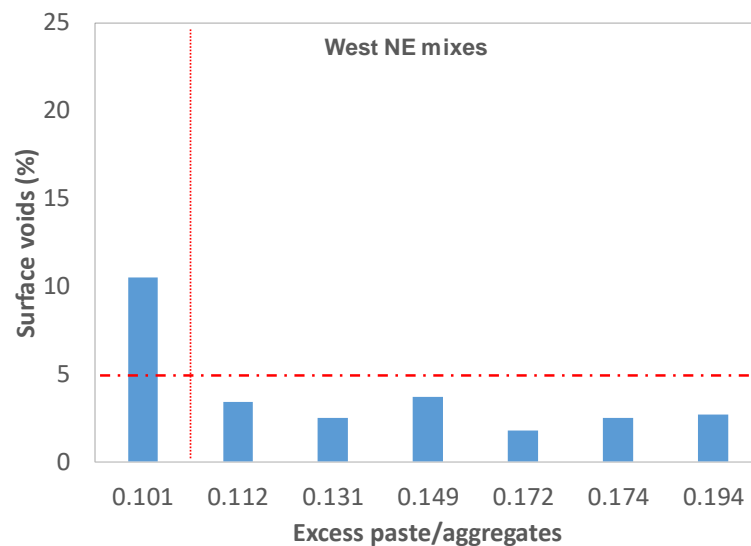
**Figure 5.1. Correlation among  $P_e\%/V_{B\_agg}\%$ ,  $V_{index}$  and surface voids**

The relationship between the calculated  $P_e\%/V_{B\_agg}\%$  ratio and surface void percentage is presented in Figure 5.2. Note that for a convenient visualization, mixtures that failed with a surface quality ranking of 4 were assigned 25% of surface voids, and mixtures that failed with an edge quality ranking of 0 were not included in the figure because it failed due to the high excess paste volume. Results showed that, based on mixes included in the present study, East NE mixtures with  $P_e\%/V_{B\_agg}\%$  ratio of 0.111 and lower resulted in a dramatic increase in surface void amount, which was deemed unacceptable. For West NE mixes, the threshold value was 0.101. The results imply that a minimum excess paste volume is required for pavement concrete to achieve sufficient performance. The reason why East NE and West NE mixtures resulted in slightly different threshold values is that the combined fineness modulus of West NE aggregates is higher, resulting in lower total surface area. The lower total surface area, the less

excess paste is required to coat aggregates (Kosmatka et al., 2008). Conservatively, a value of approximately 0.115 for East NE and 0.106 for West NE can be considered as the minimum required  $P_e\%/V_{B\_agg}\%$  ratio based on the materials included in the present study.



a) Effect of  $P_e\%/V_{B\_agg}\%$  ratio on surface voids for East NE mixes



b) Effect of  $P_e\%/V_{B\_agg}\%$  ratio on surface voids for West NE mixes

**Figure 5.2. Effect of  $P_e\%/V_{B\_agg}\%$  ratio on surface voids**

### 5.3 Proposed mix design improvement procedure

According to the results obtained and the theoretical and experimental process included in this study, a mix design improvement procedure can be recommended as shown in Figure 5.3. The first step includes obtaining an experimental packing degree of coarse and fine aggregates separately using ASTM C29 and vibration plus pressure method as discussed in the previous chapter. From the aggregate gradation results obtained per ASTM C136, the characteristic diameter of coarse and fine aggregates is obtained, which can be done by looking at the cumulative % retained and interpolating where 36.8% of particles are retained. Once individual packing degrees and characteristic diameters are known, the Modified Toufar Model should be used to obtain the optimum aggregate proportions and the packing degree of the blend. Then, the combined void content test should be performed for the selected blend, and the void contents from the aggregate skeletons can be obtained. The experimental packing degree obtained should be very close to the theoretical one. Once the aggregate blend is selected, and its void content is known, concrete can be designed with a predetermined minimum  $P_c\%/V_{B\_agg}\%$  ratio (0.106-0.115 contingent upon the combined fineness modulus) based on materials used in the present study. Afterwards, a trial concrete mix should be prepared in the lab and justified with acceptable pavement concrete performance with the Box Test in terms of surface and edge quality. An appropriate WR dosage can be applied if necessary. To account for variables such as aggregate surface texture and shape that are not directly incorporated into the current design approach, such as in the case of a mix failing the Box Test even after WR addition, concrete can be adjusted with an extra 1% of excess paste.

Then, the lab trial step is to be repeated and the mix is adjusted until an acceptable mix is obtained.

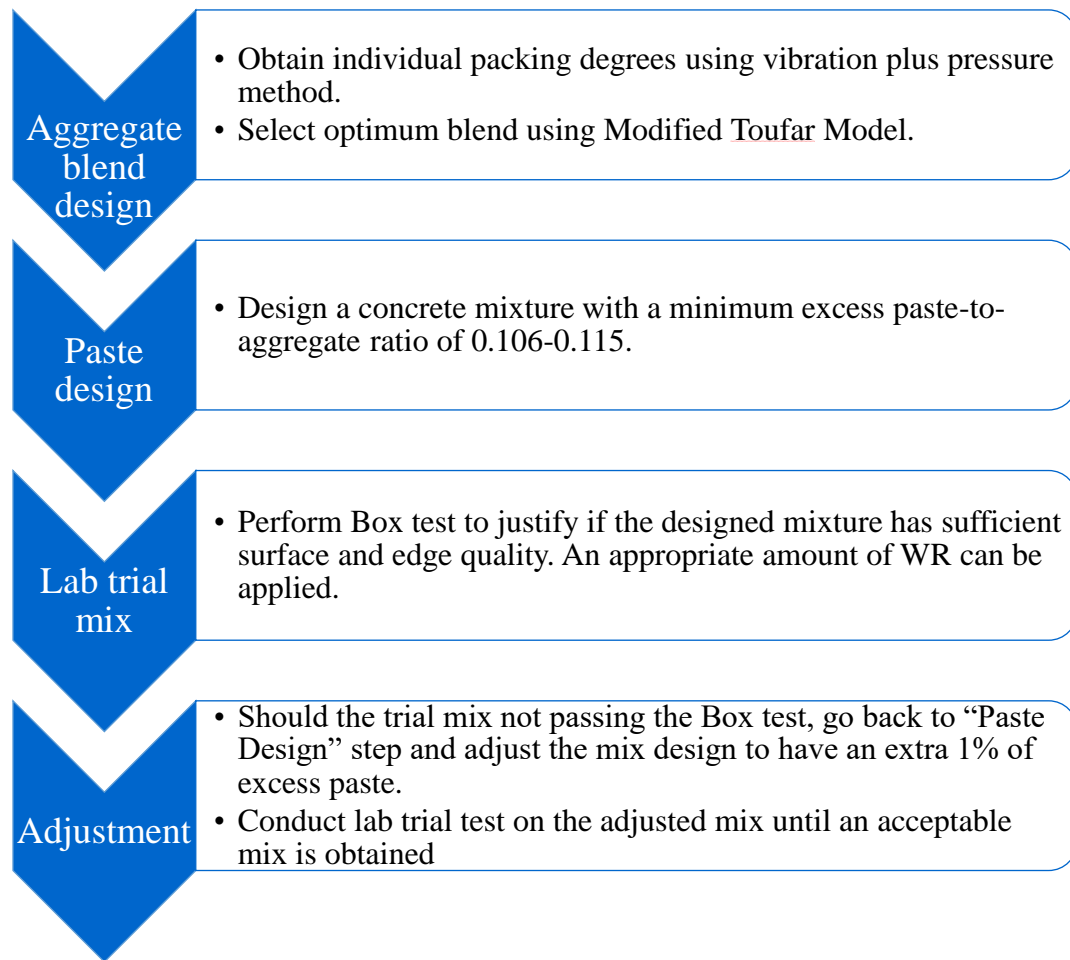


**Figure 5.3. The proposed mix design improvement procedure**

#### 5.4 Summary

Based on analysis of results of the Box Test and the VKelly Test, it was concluded that the VKelly Test is not an appropriate tool to guide the concrete design or evaluate fresh concrete with low coarse aggregate content, and only the Box Test was used to justify fresh concrete workability. Based on the Box Test results and calculated  $P_c\%/V_{B\_agg}\%$  ratio, the critical parameter of minimum required  $P_c\%/V_{B\_agg}\%$  ratio was



obtained and used for the proposed mix design improvement procedure. The first step includes aggregate blend selection based on both experimental and theoretical particle packing using the combined void content test and Modified Toufar Model. The second step required a concrete design with a minimum of  $P_c\%/V_{B\_agg}\%$  ratio of 0.106-0.115. Further steps require lab trial mix and necessary adjustments if needed. Note that the mix design improvement procedure does not account for the combined fineness modulus of the aggregate blend, which can be used as an additional criteria in future studies.

## CHAPTER 6. CONCLUSIONS AND FUTURE STUDIES

### 6.1 Conclusions

Based on results from the theoretical and experimental study of aggregate packing and the performance of pavement concrete prepared with standard and optimized aggregate gradations and reduced cement contents, the following conclusions can be drawn:

- The modified Toufar Model is an effective tool for pavement concrete mix design. Through the incorporation of the packing degree of aggregates, the model counts for the gradation, as well as the shape and texture characteristics.
- Results from the theoretical aggregate particle packing analysis based on the Modified Toufar Model matched well with the experimental results when the vibration plus pressure procedure was used.
- The Box Test with the modified index provides a reliable and more objective evaluation of the fresh pavement concrete performance. However, based on the results obtained in this study, it seems that the VKelly Test does not fit well when evaluating the performance of pavement concrete with low coarse aggregate content.
- When the optimized aggregate gradation is used, cement content can be effectively reduced by up to 1.0 sack (94 lb/yd<sup>3</sup>) without compromising the fresh properties, mechanical properties, and permeability.
- Based on the results of free and restrained shrinkage, it was justified that shrinkage and cracking potential can be reduced in concrete mixtures with optimum cement content. Freeze/thaw resistance can be slightly improved with optimized mixtures.

- A mix design improvement procedure considering both the theoretical and experimental void contents and the minimum excess paste-to-aggregate ratio ( $P_c\%/V_{B\_agg}\%$ ) can be used to design concrete with an optimum cement content.

## 6.2 Recommendations for Future Studies

### 6.2.1 Incorporation of additional parameters in mix design

The main recommendations for future studies include the incorporation of additional direct quantitative parameters to develop a more rational mix design procedure for pavement concrete. These additional parameters include direct measurement of aggregate shape and texture, combined aggregate fineness modulus, and microfines type and content.

It is believed that different aggregate blends may have comparable volumes occupying a concrete mixture and similar void content, but can differ in fineness modulus, i.e., total surface area. This difference will lead to different excess paste demand to coat aggregate particles. Therefore, the consideration of the combined fineness modulus of aggregate could be critical in mix design.

Aggregate dust is known to cause problems in concrete at different stages. It is also known that the mineralogy of the dust is crucial. For example, clay coatings have a more harmful impact on concrete performance compared to limestone dust. Clay coatings are known to weaken interfacial transition zones, thus negatively affecting strength and durability. Besides this, it was found that specific microfines can neutralize the function of AEA, and reduce entrained air significantly. Therefore, it is important to account for both amount and type of microfines.

Aggregate shape and texture are other factors not included in common mix designs directly. However, it is well known that these properties may have significant impact on both fresh and hardened concrete properties. Aggregate Image Measurement System (AIMS2) equipment can be used to determine these properties directly. The AIMS2 is an integrated machine that contains image acquisition hardware and a computer for data analysis (Figure 6.1). The equipment can provide information which includes angularity, texture, and sphericity, as well as the distribution of flat and elongated particles (Figure 6.2). The software can also provide weighted stockpile properties. These parameters can be very useful during mix design development. However, at this moment a substantial amount of experimental work is needed to obtain sufficient data to correlate these properties with fresh and hardened concrete performance. Therefore, collaboration with other state/federal agencies is necessary to collect their aggregate and concrete mix data. Moreover, incorporation of these parameters in mix design can be extended to other types of concrete, not only pavement concrete.

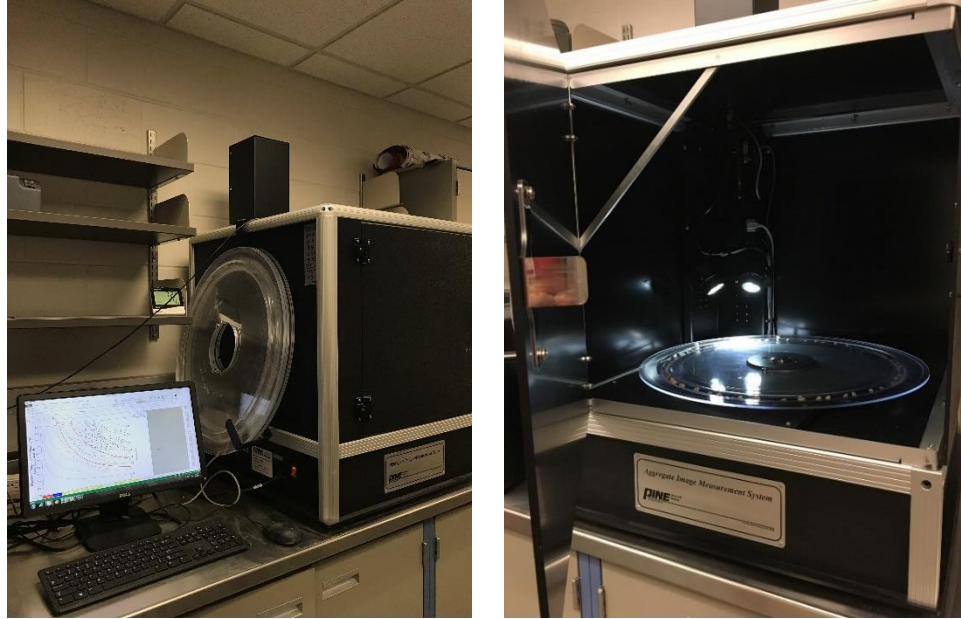


Figure 6.1. AIMS 2 setup

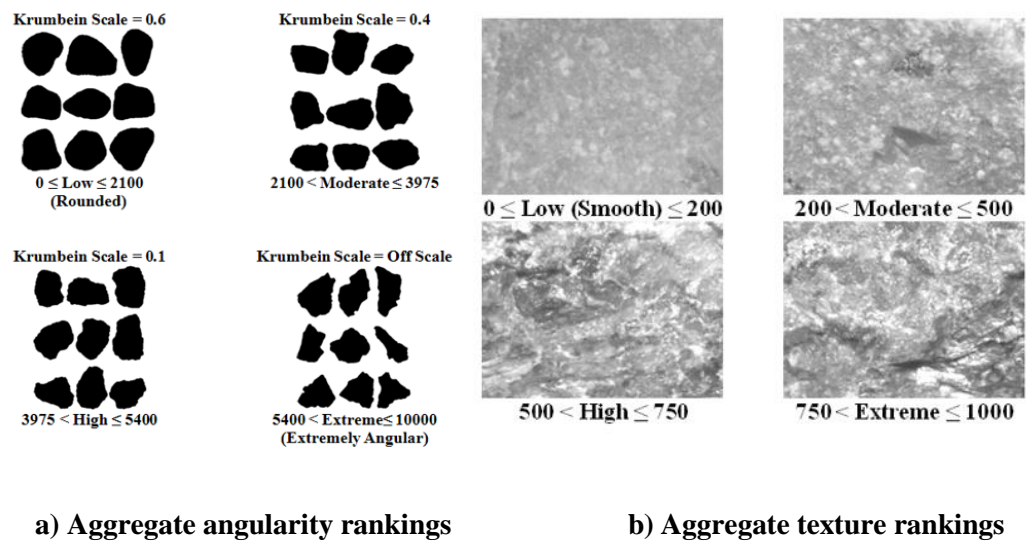


Figure 6.2. Direct measurement of aggregate shape and texture

### 6.2.2 Scientific pavement concrete workability test

Another future study might include the development of new workability tests for pavement concrete. While the slump test, Box Test, and VKelly Test are all empirical tests, a more scientific test that can effectively eliminate the human factor and provide a

completely objective measurement is needed. Concrete rheology tests can be used to characterize material flow and deformation from a scientific aspect. It is generally agreed that cement-based materials generally follow the Bingham Model (Ferraris et al., 2017), which is governed by yield stress and plastic viscosity (Figure 6.3). Rotational shear rheometers are generally used to obtain rheological properties. However, to describe slip-formed pavement concrete behavior, such rheometers need to be modified to incorporate internal or external vibration. Figure 6.4 demonstrates the sketches of a potential test setup. Both options would be suitable to use both in the laboratory and the field. It can be deduced that properties as yield stress and viscosity can describe fresh concrete behavior accurately and subjectively due to a minimized human factor.

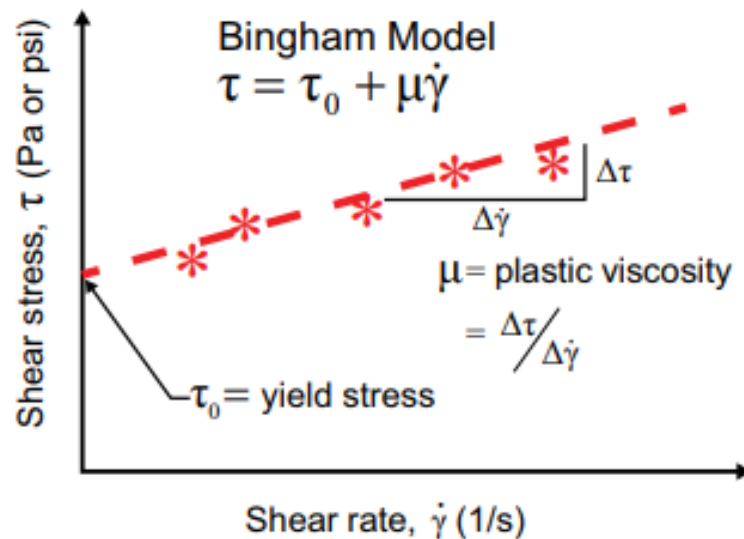
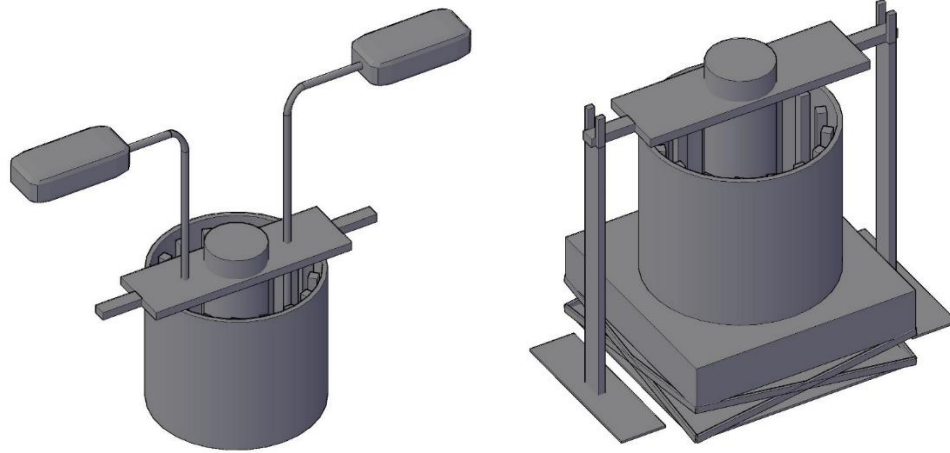


Figure 6.3. Representation of Bingham model (Ferraris et al., 2017)



**a) Rheometer with internal vibrators inserted    b) Rheometer on top of vibrating table**

**Figure 6.4. Sketch of potential new tests using rheometer and applied vibration**

## REFERENCES

AASHTO TP 95-11. Standard Method of Test for Surface Resistivity Indication of Concrete's Ability to Resist Chloride Ion Penetration. *American Association of State and Highway Transportation Officials*, 2011.

ASTM C29. Standard Test Method for Bulk Density (Unit Weight) and Voids in Aggregate. *ASTM International*, 2016.

ASTM C39. Standard Test Method for Compressive Strength of Cylindrical Concrete Specimens. *ASTM International*, 2015.

ASTM C78. Standard Test Method for Flexural Strength of Concrete (Using Simple Beam with Third-Point Loading). *ASTM International*, 2015.

ASTM C127. Standard Test Method for Relative Density (Specific Gravity) and Absorption of Coarse Aggregate. *ASTM International*, 2015.

ASTM C128. Standard Test Method for Relative Density (Specific Gravity) and Absorption of Fine Aggregate. *ASTM International*, 2015.

ASTM C136. Standard Test Method for Sieve Analysis of Fine and Coarse Aggregates. *ASTM International*, 2014.

ASTM C143. Standard Test Method for Slump of Hydraulic Cement Concrete. *ASTM International*, 2016.

ASTM C157. Standard Test Method for Length Change of Hardened Hydraulic-Cement Mortar and Concrete. *ASTM International*, 2017.



ASTM C192. Standard Practice for Making and Curing Concrete Test Specimens in the Laboratory. *ASTM International*, 2016.

ASTM C215. Standard Test Method for Fundamental Transverse, Longitudinal, and Torsional Resonant Frequencies of Concrete Specimens. *ASTM International*, 2014

ASTM C260. Standard Specification for Air-Entraining Admixtures for Concrete. *ASTM International*, 2016.

ASTM C360. Test Method for Ball Penetration in Freshly Mixed Hydraulic Cement Concrete (Withdrawn 1999). *ASTM International*, 1992.

ASTM C403. Standard Test Method for Time of Setting of Concrete Mixtures by Penetration Resistance. *ASTM International*, 2016

ASTM C469. Standard Test Method for Static Modulus of Elasticity and Poisson's Ratio of Concrete. *ASTM International*, 2014

ASTM C494. Standard Specification for Chemical Admixtures for Concrete. *ASTM International*, 2017.

ASTM C595. Standard Specification for Blended Hydraulic Cements. *ASTM International*, 2018.

ASTM C666. Standard Test Method for Resistance of Concrete to Rapid Freezing and Thawing. *ASTM International*, 2015

ASTM C1581. Standard Test Method for Determining Age at Cracking and Induced Tensile Stress Characteristics of Mortar and Concrete under Restrained Shrinkage. *ASTM International*, 2018

- Andrew, R.M. *Global Co2 Emissions from Cement Production*. Earth System Science Data, 2018, 10: 195-217.
- Cook, D., Ley, T., and Ghaeezadah, A. A Workability Test for Slip Formed Concrete Pavements. *Construction and Building Materials*, 2014, 68: 376-383.
- Cook, D., Ley, T., Ghaeezadah, A. *Effects of Aggregate Concepts on the Workability of Slip-Formed Concrete*. Journal of Materials in Civil Engineering, 2016, 28-10.
- De Larrard, F. *Concrete Mixture Proportioning: a scientific approach*. Taylor & Francis, New York, 1999.
- Ferrais, C.F., Billberg, P., Ferron, R., Feys, D., Hu, J., Kawashima, S., Koehler, E., Sonebi, M., Tanesi, J., Tregger, N. *Role of Rheology in Achieving Successful Concrete Performance*. Concrete International, 2017, 39-6: 43-51.
- Furnas, C.C. Sun. *Flow of Gases Through Beds of Broken Solids*. Bureau of Mines, United States. 1928.
- Goltermann, P., Johansen, V., Palbol, L. Packing of Aggregates: An Alternative Tool to Determine the Optimal Aggregate Mix. *ACI Materials Journal*, 1997, 94-M51: 435-442.
- Heyen, W., Halsey, L. *Optimized Aggregates Gradations for Portland Cement Concrete Mix Designs Evaluation*. Nebraska Department of Roads, 2013.
- Jones, M.R., Zheng, L., Newlands, D.D. *Comparison of Particle Packing Models for Proportioning Concrete Constituents for Minimum Voids Ratio*. Materials and Structures, 2002, 35: 301-309.

Kennedy, C.T. The design of concrete mixes. *Journal of the American Concrete Institute*, 1940, 36: 373-400

Kwan, A.K.H., Mora, C.F. *Effects of Various Shape Parameters on Packing of Aggregate Particles*. Magazine of Concrete Research, 2001, 53-2: 91-100.

Kosmatka, S., Kerkhoff, B., Panarese, W. *Design and Control of Concrete Mixtures, 14th Edition*. Portland Cement Association, Skokie, IL, 2008.

Lamond, J.F., Pielert, J.H. *Significance of Tests and Properties of Concrete and Concrete-Making Materials*. ASTM International, 2006, STP169D.

Ley, T., Cook, D., and Fick, G. *Concrete Pavement Mixture Design and Analysis (MDA): Effect of Aggregate Systems on Concrete Properties*. National Concrete Pavement Technology Center, Ames, IA, 2012.

Ley, T. and Cook, D. *Aggregate Gradations for Concrete Pavement Mixtures*. CP 9 Road Map. Moving Advancements into Practice (MAP) Brief. FHWA TPF-5-(286), 2014.

Mangulkar, M.N, Jamkar, S.S. *Review of Particle Packing Theories Used for Concrete Mix Proportioning*. International Journal of Scientific & Engineering Research, 2013, 4-5: 143-148.

Moini, M. *The Optimization of Concrete Mixtures for Use in Highway Applications*. Master Thesis, The University of Wisconsin-Milwaukee, 2015.

Obla, K., Kim, H., Lobo, C. *Effect of Continuous (Well-Graded) Combined Aggregate Grading on Concrete Performance Phase A: Aggregate Voids Content (Packing Density)*. National Ready Mix Concrete Association, 2007.

Obla, K. (2011). *Variation in Concrete Performance due to aggregates*. Concrete infocus: a publication of the national ready mixed concrete association, 2011, 10-5: 9-14.

Quiroga, P.N. and Fowler, D.W. *The Effects of Aggregates Characteristics on the Performance of Portland Cement Concrete*. Report ICAR 104-1F. International Center for Aggregates Research, University of Texas at Austin, 2004.

Rached, M., De Moya, M., Fowler, D.W. *Utilizing Aggregates Characteristics to Minimize Cement Content in Portland Cement Concrete*. International Center for Aggregate Research, 2009.

Ramakrishnan, V. *Optimized Aggregate Gradation for Structural Concrete*. South Dakota Department of Transportation, 2004.

Rudy, A.K. *Optimization of Mixture Proportions for Concrete Pavements - Influence of Supplementary Cementitious Materials, Paste Content and Aggregate Gradation*. Ph.D. Dissertation, Purdue University, 2009.

Siddiqui, M.S., Rached, M., and Fowler, D. *Rational Mixture Design for Pavement Concrete*. Transportation Research Record: Journal of the Transportation Research Board, 2014, 2441: 20-27.

Standard Specifications for Highway Construction. Nebraska Department of Transportation, 2017.

Stovall, T., de Larrard, F., Buil, M. *Linear Packing Density Model of Grain Mixtures*. Powder Technology, 1986, 48: 1-12.

Taylor, P., Bektas, F., Yurdakul, E., Ceylan, H. *Optimizing Cementitious Content in Concrete Mixtures for Required Performance*. National Concrete Pavement Technology Center, Ames, IA, 2012.

Taylor, P., Yurdakul, E., Wang, X., Wang, X. *Concrete Pavement Mixture Design and Analysis (MDA): An Innovative Approach to Proportioning Concrete Mixtures*. National Concrete Pavement Technology Center, Ames, IA, 2015.

Taylor, P. *Blended Aggregates for Concrete Mixture Optimization: Best Practices for Jointed Concrete Pavements*. FHWA-HIF-019, 2015.

Taylor, P., Wang, X., Wang, X. *Concrete Pavement Mixture Design and Analysis (MDA): Development and Evaluation of Vibrating Kelly Ball Test (VKelly Test) for the Workability of Concrete*. National Concrete Pavement Technology Center, Ames, IA, 2015.

Wang, X., Wang, K., Taylor, P., Morcou, G. *Assessing Particle Packing Based Self-consolidating Concrete Mix Design Method*. *Construction and Building Materials*, 2014, 70: 439-452.

Wassermann, R., Katz, A., Bentur, A. *Minimum cement content requirements: a must or a myth?*. *Materials and Structures*, 2009, 42: 973–982.

Yurdakul, E. *Optimizing concrete mixtures with minimum cement content for performance and sustainability*. Master thesis, Iowa State University, 2010.